



Kent Academic Repository

Sayer, Andrew P., Llaverro-Pasquina, Marcel, Geisler, Katrin, Holzer, Andre, Bunbury, Freddy, Mendoza-Ochoa, Gonzalo I., Lawrence, Andrew D., Warren, Martin J., Mehrshahi, Payam and Smith, Alison G. (2023) *Conserved cobalamin acquisition protein 1 is essential for vitamin B12 uptake in both Chlamydomonas and Phaeodactylum*. *Plant Physiology*, 194 (2). pp. 698-714. ISSN 0032-0889.

Downloaded from

<https://kar.kent.ac.uk/103388/> The University of Kent's Academic Repository KAR

The version of record is available from

<https://doi.org/10.1093/plphys/kiad564>

This document version

Author's Accepted Manuscript

DOI for this version

Licence for this version

CC BY (Attribution)

Additional information

For the purpose of open access, the author has applied a CC BY public copyright licence to any Author Accepted Manuscript version arising from this submission.

Versions of research works

Versions of Record

If this version is the version of record, it is the same as the published version available on the publisher's web site. Cite as the published version.

Author Accepted Manuscripts

If this document is identified as the Author Accepted Manuscript it is the version after peer review but before type setting, copy editing or publisher branding. Cite as Surname, Initial. (Year) 'Title of article'. To be published in **Title of Journal**, Volume and issue numbers [peer-reviewed accepted version]. Available at: DOI or URL (Accessed: date).

Enquiries

If you have questions about this document contact ResearchSupport@kent.ac.uk. Please include the URL of the record in KAR. If you believe that your, or a third party's rights have been compromised through this document please see our [Take Down policy](https://www.kent.ac.uk/guides/kar-the-kent-academic-repository#policies) (available from <https://www.kent.ac.uk/guides/kar-the-kent-academic-repository#policies>).

1 **RESEARCH ARTICLE**

2
3
4 **Conserved cobalamin acquisition protein 1 is essential for vitamin B₁₂**
5 **uptake in both *Chlamydomonas* and *Phaeodactylum***

6
7 Andrew P. Sayer^{1*}, Marcel Llaveró-Pasquina^{1¶}, Katrin Geisler¹, Andre Holzer^{1‡}, Freddy Bunbury^{1§},
8 Gonzalo I. Mendoza-Ochoa¹, Andrew D. Lawrence², Martin J. Warren^{3,4}, Payam Mehrshahi¹, Alison
9 G. Smith^{1*}

10 ¹Department of Plant Sciences, University of Cambridge, Downing Street, Cambridge, CB2 3EA, UK

11 ²School of Biological Sciences, University of Southampton, Southampton SO17 1BJ, UK

12 ³School of Biosciences, University of Kent, Canterbury, Kent, CT2 7NJ, UK

13 ⁴Quadram Institute Bioscience, Norwich Research Park, Norwich, NR4 7UA, UK

14
15 **Current addresses:**

16 * CRUK-AZ Functional Genomics Centre, Milner Therapeutics Institute, University of Cambridge,
17 Puddicombe Way, Cambridge, CB2 0AW, UK

18 ¶ Environmental Science and Technology Institute (ICTA-UAB), Universitat Autònoma de Barcelona
19 (UAB) 08193 Bellaterra (Cerdanyola del Vallès) - Spain

20 ‡ Center for Bioinformatics and Department of Computer Science, Saarland University, Saarbrücken,
21 Germany

22 § Department of Plant Biology, Carnegie Science, 260 Panama Street, Stanford CA 94305, USA

23
24 * **Author for correspondence:** Alison Smith

25 Email: as25@ cam.ac.uk; orcid.org/0000-0001-6511-5704;

26 Phone: +44-1223 333952; Fax: +44-1223 333953

27 The author responsible for distribution of materials integral to the findings presented in this article in
28 accordance with the policy described in the Instructions for Authors
29 (<https://academic.oup.com/plphys/pages/General-Instructions>) is Alison Smith (as25@ cam.ac.uk).

30 **Short title:** Identification of a B₁₂ uptake protein in algae

31
32 **One sentence summary:** Knockout mutants and physiological studies demonstrate that vitamin B₁₂
33 uptake in both *Chlamydomonas reinhardtii* and the unrelated *Phaeodactylum tricorutum* requires
34 cobalamin acquisition protein 1.

35
36 **Keywords:** cobalamin, *Chlamydomonas reinhardtii*, *Phaeodactylum tricorutum*, insertional
37 mutagenesis, CLiP mutants, CRISPR-Cas9, riboswitch

38
39 **Manuscript length:** 7241 words

40 **Abstract**

41

42 Microalgae play an essential role in global net primary productivity and global biogeochemical
43 cycling. Despite their phototrophic lifestyle, over half of algal species depend for growth on acquiring
44 an external supply of the corrinoid vitamin B₁₂ (cobalamin), a micronutrient produced only by a
45 subset of prokaryotic organisms. Previous studies have identified protein components involved in
46 vitamin B₁₂ uptake in bacterial species and humans. However, little is known about its uptake in
47 algae. Here, we demonstrate the essential role of a protein, cobalamin acquisition protein 1 (CBA1),
48 in B₁₂ uptake in *Phaeodactylum tricornutum* using CRISPR-Cas9 to generate targeted knockouts and
49 in *Chlamydomonas reinhardtii* by insertional mutagenesis. In both cases, CBA1 knockout lines could
50 not take up exogenous vitamin B₁₂. Complementation of the *C. reinhardtii* mutants with the wild-type
51 *CBA1* gene restored B₁₂ uptake, and regulation of *CBA1* expression via a riboswitch element enabled
52 control of the phenotype. When visualised by confocal microscopy, a YFP-fusion with *C. reinhardtii*
53 CBA1 showed association with membranes. Bioinformatics analysis found that CBA1-like sequences
54 are present in all major eukaryotic phyla. In algal taxa, the majority that encoded CBA1 also had
55 genes for B₁₂-dependent enzymes, suggesting CBA1 plays a conserved role. Our results thus provide
56 insight into the molecular basis of algal B₁₂ acquisition, a process that likely underpins many
57 interactions in aquatic microbial communities.

58 INTRODUCTION

59

60 Microalgae are a diverse group of eukaryotic organisms that thrive in all aquatic environments. They
61 form the basis of most aquatic food chains and are major contributors to global primary productivity,
62 with marine microalgae responsible for an estimated 30% of total carbon fixation (Field et al., 1998).
63 Understanding the drivers that support algal growth is thus of considerable ecological importance.
64 Despite their photoautotrophic lifestyle, a widespread trait in algae is dependence on an external
65 source of an organic micronutrient, vitamin B₁₂ (cobalamin), a complex cobalt-containing corrinoid
66 molecule. Approximately half of algal species surveyed across the eukaryotic tree of life require B₁₂
67 for growth (Croft et al., 2005). However, the proportion of B₁₂-dependent species differs between
68 algal groups, from 30% (n=148) of Chlorophytes to 96% (n=27) of algal species that participate in
69 harmful algal blooms (Tang et al., 2010). Within algal lineages, there is no evidence that any can
70 produce B₁₂ *de novo*, so this auxotrophy is not due to loss of one or more biosynthetic genes. Rather,
71 the requirement for B₁₂ stems from the fact that it is an essential cofactor for methionine synthase
72 (METH), and species that can grow without supplementation have an alternative, B₁₂-independent,
73 isoform of this enzyme called METE (Croft et al., 2005; Helliwell et al., 2011). Many microalgae,
74 including the green alga *Chlamydomonas reinhardtii* and the unrelated diatom *Phaeodactylum*
75 *tricornutum*, encode both forms of methionine synthase and utilise METE in the absence of
76 exogenous B₁₂, but take up and utilise the compound if it becomes available (Helliwell et al., 2011).
77 Under those conditions, the expression of *METE*, which has been found to have a lower catalytic rate
78 than *METH* (Gonzalez et al. 1992), is repressed, and cells rely on *METH* activity.

79

80 The biosynthetic pathway for B₁₂ is confined to prokaryotes (Warren et al., 2002) and indeed only a
81 subset of bacteria encode the entire set of 20 or so enzymes required to synthesise corrinoids from the
82 common tetrapyrrole precursor (Shelton et al., 2019), with many eubacterial species also reliant on an
83 external source. In some cases, this is due to the loss of one or a few enzymes of the biosynthetic
84 pathway, but in many bacteria the pathway is absent altogether and auxotrophy is the consequence of
85 relying on one or more B₁₂-dependent enzymes, such as *METH*. In microalgae, supplementation of
86 cultures of *P. tricornutum* with B₁₂ increases its growth rate subtly (Bertrand et al., 2012) and in *C.*

87 *reinhardtii* use of METH confers thermal tolerance (Xie et al., 2013). More direct evidence for a
88 selective advantage is demonstrated by the fact that an experimentally-evolved *metE* mutant of *C.*
89 *reinhardtii* predominates in mixed populations with wild-type cells over tens of cell generations, as
90 long as B₁₂ is included in the medium (Helliwell et al., 2015). This is despite the fact that in the
91 absence of B₁₂, the *metE* mutant is non-viable within a few days (Bunbury et al., 2020).

92
93 The minimum levels of B₁₂ in the medium needed to support growth of laboratory cultures of algal
94 B₁₂-auxotrophs are in the range of 10-50 pM (Croft et al., 2005), whereas B₁₂ concentrations have
95 been reported to be just 5-13 pM in freshwater systems (Ohwada, 1973). A similar value of 6.2 pM is
96 the average value in most marine environments, although up to 87 pM could be detected in some
97 coastal waters (Sañudo-Wilhelmy et al., 2014), which may be linked to the higher cobalt
98 concentrations measured there (Panzeca et al., 2009). Given the limiting levels of B₁₂ in the
99 environment, its relatively short half-life (in the order of days) in surface water (Carlucci et al., 2007;
100 Sañudo-Wilhelmy et al., 2014), and that as a large polar molecule it is unlikely to simply diffuse
101 across cellular membranes, it is clear that algae must have an efficient means to take up B₁₂. In
102 bacteria, the molecular mechanisms for B₁₂ uptake have been extensively characterised. The B₁₂
103 transport and utilisation (*btu*) operon is perhaps the best known (Kadner, 1990), comprising BtuB, a
104 TonB-dependent transporter in the outer membrane, a B₁₂-binding protein, BtuF, located in the
105 periplasm, and BtuC and BtuD, components of an ATP-binding cassette (ABC) transporter that sits in
106 the inner membrane (Borths et al., 2002). In mammals, dietary B₁₂ is bound to intrinsic factor in the
107 ileum and taken up from the gut via receptor-mediated endocytosis (Nielsen et al., 2012). It is then
108 transported between and within cells via multiple B₁₂ transport proteins (Banerjee et al., 2021; Choi
109 and Ford, 2021). These include lipocalin-1 interacting membrane receptor domain-containing protein
110 1 (LMBD1), ATP-binding cassette subfamily D member 4 (ABCD4), the latter being an integral
111 membrane ABC transporter in the lysosomal membrane of gut epithelial cells, which facilitates
112 delivery of B₁₂ into the cytosol, and multidrug resistant protein 1 (MRP1, also known as ABCC1),
113 another ABC transporter that has sequence similarity to BtuCD and is involved in export of free B₁₂
114 into the plasma where it binds to the main B₁₂ transport protein, transcobalamin (Beedholm-Ebsen et

115 al., 2010). Mice *mrp1* mutants were still able to transport a small amount of cobalamin out of cells,
116 indicating redundant mechanisms for this function that have not yet been identified. Cobalamin
117 circulating in the plasma bound to transcobalamin can then be taken up by other cells via receptor-
118 mediated endocytosis (Nielsen et al., 2012).

119

120 In contrast to these well-studied processes in bacteria and mammals, the understanding of B₁₂
121 acquisition in microalgae is more limited. A survey of microalgal species, including marine and
122 freshwater taxa and those that require B₁₂ (for example *Euglena gracilis*, *Thalassiosira pseudonana*)
123 and non-requireers (such as *P. tricornutum*, *Dunaliella primolecta*), found that many released a ‘B₁₂-
124 binder’ into the medium, likely a protein, that appeared to sequester B₁₂ from solution and thereby
125 inhibited growth of B₁₂-dependent algae (Pintner and Altmeyer, 1979). Its role was unknown, but it
126 was postulated that it might be involved in competition for resources between microalgal species in
127 the environment. Subsequently, a protein was purified from the medium of cultures of *T. pseudonana*
128 with a high affinity binding constant of 2 pM for B₁₂ (Sahni et al., 2001). In its native state it was an
129 oligomer of >400 kDa, with subunits of ~80 kDa and the amino acid profile was determined, but it
130 was not possible to obtain sufficient amounts to characterise further. A different approach was taken
131 by Bertrand et al. (2012), who conducted a transcriptomics and proteomics study of *P. tricornutum*
132 and *T. pseudonana* grown under low or sufficient B₁₂ conditions. This led to the identification of a
133 gene highly upregulated at the transcript and protein level in the absence of B₁₂. Overexpression of
134 this protein in *P. tricornutum* resulted in an increase in the rate of B₁₂ uptake, and the protein was
135 named CoBalamin Acquisition protein 1 (CBA1) although no direct role was established. In this study
136 we have taken a mutagenesis approach to identify genes responsible for B₁₂ uptake in both *P.*
137 *tricornutum* and *C. reinhardtii*, including extending the work on CBA1. In addition, we have
138 determined the extent to which candidate proteins are conserved throughout the algal lineages,
139 making use of recent increases in algal sequencing data.

140 RESULTS

141

142 *P. tricornutum* CBA1 knockout lines do not take up B₁₂

143 Previous work showed that overexpression of CBA1 in *P. tricornutum* conferred enhanced B₁₂ uptake
144 rates (Bertrand et al., 2012) but the study did not demonstrate whether it was essential for this process.
145 To address this question, CBA1 knockout lines were generated in *P. tricornutum* strain 1055/1
146 (Supplemental Table S1) by CRISPR-Cas9 editing, using a homologous recombination repair
147 template that included a nourseothricin resistance (*NAT*) cassette (Figure 1a). CRISPR-Cas9 lines
148 were cultured on selective media and screened for the absence of WT alleles at the *PtCBA1* locus
149 (Phatr3_J48322) using PCR (Figure 1b). When the *PtCBA1* gene was amplified (top panel, Figure 1b)
150 from Δ CBA1-1 with primers flanking the homologous recombination regions, two bands were
151 detected; the larger of these corresponded to the WT amplicon, whilst the smaller band corresponded
152 to a replacement of CBA1 by *NAT*, suggesting that this strain is a mono-allelic knockout. For Δ CBA1-
153 2, the *PtCBA1* gene primers amplified a single smaller product, suggesting that this was a bi-allelic
154 knockout, whereas the *PtCBA1* ORF primers (bottom panel of Figure 1b) did not amplify anything,
155 indicating a disruption specifically in this region. Similarly, no band was detected with primers that
156 amplify across the 5' end of the *NAT* knock-in (HR primers), which might indicate further disruptions
157 upstream of the 5'HR region of Δ CBA1-2. Although a larger band than for WT was amplified in
158 Δ CBA1-3 using the *PtCBA1* gene primers, those for the *PtCBA1* ORF amplified a smaller product; in
159 both cases a single band was observed indicating a bi-allelic deletion at the sgRNA target sites.

160

161 To test whether the Δ CBA1 lines were affected in their ability to take up vitamin B₁₂ we developed a
162 standardised B₁₂-uptake assay, detailed in Materials and Methods. In brief, algal cells were grown to
163 the same growth stage and adjusted to the same cell density, then incubated in media containing a
164 known amount of cyanocobalamin for one hour. Thereafter, cells were pelleted by centrifugation and
165 the amount of B₁₂ determined in the cell pellet and the media fraction using a *Salmonella typhimurium*
166 bioassay (Bunbury et al., 2020). For each sample, the B₁₂ measured in the cellular and media fractions
167 were added to provide an estimated 'Total' and compared to the amount of B₁₂ added initially (Figure

168 1c, dashed line), to determine the extent of recovery. For the WT strain, most of the added B₁₂ was
169 found in the cellular fraction. The mono-allelic knockout line ΔCBA1-1 consistently showed ~20-
170 30% B₁₂ uptake relative to the WT strain. This suggested that a single copy of *PtCBA1* is sufficient to
171 confer B₁₂ uptake in *P. tricornutum*, but not to the same extent as the WT strain. In contrast, for the
172 two bi-allelic knockout lines (ΔCBA1-2 and ΔCBA1-3) no B₁₂ was detected in the cellular fraction in
173 any experiment, indicating that vitamin B₁₂ uptake was fully impaired in the absence of a functional
174 *PtCBA1* copy, at least at the limit of detection of the B₁₂ bioassay (of the order of 10 pg). These
175 results expand our understanding of *PtCBA1* by demonstrating that its presence is essential for B₁₂
176 uptake and indicates that there is no functional redundancy to *PtCBA1*.

177

178 **Insertional mutagenesis identified the *C. reinhardtii* homologue of *CBA1***

179 Bertrand et al. (2012) reported that there were no detectable *CBA1* homologues in algal lineages
180 outside the Stramenopiles, so to investigate B₁₂ uptake in *C. reinhardtii*, we decided to take an
181 insertional mutagenesis approach. We took advantage of the fact that B₁₂ represses expression of the
182 *METE* gene at the transcriptional level via the promoter (P_{METE}), and that reporter genes driven by this
183 genetic element respond similarly (Helliwell et al., 2014), to develop a highly sensitive screen for
184 lines no longer able to respond to B₁₂. We hypothesised that, since P_{METE} is likely to respond
185 specifically to intracellular B₁₂, P_{METE} would not be repressed in strains unable to take up B₁₂ from the
186 media, so the reporter would be expressed and functional. If the reporter were an antibiotic resistance
187 gene, this would allow identification of B₁₂ uptake mutants in a more high-throughput manner than
188 the B₁₂-uptake assay. The background strain for insertional mutagenesis was made by transforming *C.*
189 *reinhardtii* strain UVM4 (Neupert et al., 2009) with plasmid pAS_R1 containing a paromomycin
190 resistance gene (*aphVIII*) under control of P_{METE} (Figure 2a, top construct; Supplemental Table S2).
191 Lines of this strain were tested for their responsiveness to B₁₂ and paromomycin. One line, UVM4-
192 T12, showed the appropriate sensitivity with increasing repression of growth in paromomycin as B₁₂
193 concentrations were increased, the effect being more marked at 15-20 μg·ml⁻¹ paromomycin than at 5-
194 10 μg·ml⁻¹ (Figure 2b). This line thus allowed for an easily quantifiable growth phenotype that was
195 proportionally related to B₁₂ concentration.

196

197 Insertional mutagenesis was carried out by transforming UVM4-T12 with a plasmid (pHyg3)
198 containing a hygromycin resistance gene (*aphVII*) under the control of the constitutively expressed
199 β 2-tubulin promoter (Figure 2a, bottom construct), generating a population of UVM4-T12::pHyg3
200 lines with the cassette randomly inserted into the nuclear genome. By plating the products of the
201 transformation on solid TAP media supplemented with a range of paromomycin, hygromycin and
202 vitamin B₁₂ concentrations (see Methods), 7 colonies were obtained. This was estimated to be from
203 approximately 5000 primary transformants, determined by plating the same volume on TAP plates
204 with the antibiotics but without B₁₂. These 7 putative insertional mutant (IM) lines were then assessed
205 for their ability to take up B₁₂ using the B₁₂ uptake assay. For UVM4, UVM4-T12 and insertional
206 lines from the plate without B₁₂ (labelled Control 1-3), similar amounts of B₁₂ were recovered from
207 the cellular and media fractions (Supplemental Figure S1). This was also the case for 6 of the IM
208 lines, suggesting that they could still take up B₁₂ and were likely false positives of the initial screen.
209 However, no B₁₂ could be detected in the cellular fraction of UVM4-T12::pHyg3 #IM4 (hereafter
210 referred to as IM4), indicating that this mutant line did not take up B₁₂.

211

212 To obtain independent corroboration that IM4 was impaired in B₁₂ uptake, cells of this mutagenized
213 line were incubated with a fluorescently-labelled B₁₂ derivative, B₁₂-BODIPY (Lawrence et al., 2018),
214 and then imaged using confocal microscopy. *C. reinhardtii* cells were incubated in TAP medium
215 without B₁₂-BODIPY or with 1 μ M B₁₂-BODIPY for 1 hour, washed with fresh media and
216 subsequently imaged. There was no signal detected in the channel used for B₁₂-BODIPY (589 nm
217 excitation; 607-620 nm detection) in samples without B₁₂-BODIPY added (Supplemental Figure S2,
218 top two rows), indicating that the imaging protocol was specific to this compound. When B₁₂-
219 BODIPY was added, UVM4-T12 showed the B₁₂-BODIPY signal located within the algal cell
220 (Supplemental Figure S2, third row), indicating that this signal could be effectively detected by the
221 imaging protocol and that B₁₂-BODIPY was being transported into the cells. In contrast, there was no
222 B₁₂-BODIPY signal in IM4 cells, supporting the hypothesis that B₁₂ uptake was impaired in this
223 mutant (Supplemental Figure S2, bottom row). In addition, the response of the *METE* gene to B₁₂ in

224 IM4 was assessed by RT-qPCR. UVM4 and IM4 cultures were grown in media with or without
225 addition of B₁₂ for 4 days in continuous light, after which the cultures were harvested for RNA
226 extraction and cDNA synthesis. As expected, *METE* was repressed in UVM4 in the presence of B₁₂
227 compared to no supplementation (Figure 3a), whereas IM4 showed similar *METE* expression in both
228 conditions. This provided further support for disrupted B₁₂ uptake in this line.

229

230 To identify the genomic location of the causal mutation in IM4, short-read whole genome sequencing
231 was performed on DNA samples from UVM4, UVM4-T12 and IM4. The location of the pHyg3
232 cassette in IM4 was identified as described in Methods and found to have disrupted the
233 *Cre12.g508644* locus (Supplemental Figure S3a), an unannotated gene. To corroborate that disruption
234 of the *Cre12.g508644* was responsible for the uptake-phenotype, two independent mutant lines of the
235 gene (LMJ-119922 and LMJ-042227) were ordered from the Chlamydomonas library project (CLiP)
236 collection (Li et al., 2016) and verified to be disrupted at this locus by PCR (Supplemental Figure
237 S3a). However, when these knockout lines were tested for the ability to take up B₁₂ using the B₁₂
238 uptake assay, they were both found to be able to do so to a similar extent as their parental strain, cw15
239 (Figure S3b). This suggested that *Cre12.g508644* did not encode a protein essential for B₁₂ uptake.

240

241 We therefore examined the genome sequence data more closely to determine the genetic cause for the
242 B₁₂-uptake phenotype of IM4. We had identified putative homologues of human proteins involved in
243 receptor-mediated endocytosis of B₁₂, such as ABCD4, LMBD1 (Rutsch et al., 2009; Coelho et al.,
244 2012) and MRP1 (Beedholm-Ebsen et al., 2010), in the *C. reinhardtii* genome by BLAST. However,
245 given the widespread percentage of SNPs in the IM4 genome compared to UVM4, it was not possible
246 to identify any candidate causal mutations with confidence. Instead, manual inspection of the DNA
247 sequencing reads mapped to the reference strain revealed one locus, *Cre02.g081050*, annotated as
248 flagella-associated protein 24 (FAP24), where there was a unique discontinuity, suggesting that there
249 was an insertion at exon 2 in IM4 (Figure 3b; Supplemental Figure S4a). The sequence was bordered
250 by a genome duplication of 8 bp (shown in blue in Figure S4a) and exhibited imperfect inverted
251 repeats at the terminal regions (TIRs), indicative of a transposable element. Reads could not be

252 assembled across the discontinuity to obtain the complete sequence of the insertion, but using the left
253 and right junction sequences as queries, three regions encoding two very similar genes were identified
254 (Supplemental Figure S4b).

255
256 Remarkably, when the *Cre02.g081050* protein was used as a query in a BLAST search, one of the hits
257 recovered was the PtCBA1 protein (22.9% sequence identity), even though the reciprocal sequence
258 search had not picked up the *C. reinhardtii* gene (Bertrand et al., 2012). Predicted 3D structures of
259 PtCBA1 and the *C. reinhardtii* protein encoded by *Cre02.g081050* were obtained from the
260 AlphaFold2 protein structure database and overlaid (Supplemental Figure S5). The modelled proteins
261 showed a high degree of structural similarity to one another (root mean squared deviation (RMSD) =
262 1.688), particularly with respect to the arrangement of alpha helices and a lower cleft. Due to the
263 sequence similarity and predicted structural similarity, these proteins appeared to be homologous to
264 one another and *Cre02.g081050* is hereafter referred to as CrCBA1.

265
266 To determine whether disruption of *CrCBA1* in IM4 was responsible for the impaired B₁₂ uptake, we
267 investigated whether it was possible to restore its ability to take up B₁₂ by transforming IM4 with the
268 wild-type *CrCBA1*. Construct pAS_C2 was designed with the *CrCBA1* promoter, *CrCBA1* open
269 reading frame (ORF) and terminator and included a 3' mVenus tag attached by a poly-glycine linker
270 (Figure 3c). IM4 was transformed with pAS_C2, and resulting lines were tested for the ability to take
271 up B₁₂ using the B₁₂ uptake assay. As observed previously, UVM4 was able to take up B₁₂ whilst IM4
272 was unable to do so (Figure 3d). The CBA1 complementation line IM4::pAS_C2 showed B₁₂ in the
273 cellular fraction at similar levels as in UVM4, thereby indicating that the mutant phenotype had been
274 complemented.

275
276 ***CrCBA1* CLiP mutant is unable to take up B₁₂ and is complemented by the WT *CrCBA1* gene**

277 Given the many genetic changes in line IM4 compared to the parental UVM4-T12 strain caused by
278 the mutagenesis, it was essential to have independent corroboration that mutation of *CrCBA1* caused
279 the inability to take up B₁₂. Accordingly, we obtained two further CLiP mutants (LMJ-135929 and

280 LMJ-040682) with disruptions in intron 2 and introns 6/7 respectively of *CrCBA1* (Supplemental
281 Figure S6a) and assessed them for their ability to take up B₁₂ (Supplemental Figure S6b). No B₁₂ was
282 detected in cells of LMJ-040682, indicating complete inhibition of B₁₂ uptake. Although LMJ-135929
283 cells accumulated some B₁₂, this was less than half the amount of its parent strain cw15, suggesting
284 partial impairment in uptake, similar to the phenotype of the monoallelic *PtCBA1* knockout line
285 (Figure 1c). However, heterozygosity cannot be the explanation for *C. reinhardtii*, which is haploid,
286 and instead indicates that LMJ-135929 was likely to have just partial knockdown of the gene,
287 probably because the insertion is in an intron.

288

289 Nonetheless, to provide further confirmation that mutations in *CrCBA1* were responsible for the
290 observed impaired B₁₂ uptake, we again tested whether the phenotype could be complemented with
291 the wild-type *CrCBA1* gene using both plasmid pAS_C2 (Figure 3b) and an additional construct
292 pAS_C3 (Figure 4a), in which expression of *CrCBA1* can be controlled by a thiamine pyrophosphate
293 (TPP) repressible riboswitch, RS_{THI4_AN} (Mehrshahi et al., 2020). In the absence of thiamine
294 supplementation of the cultures, the riboswitch is not active and the gene containing it is transcribed
295 and translated as normal; with thiamine addition, alternative splice sites are utilised, leading to
296 inclusion of an upstream ORF containing a stop codon in the mRNA, preventing translation from the
297 downstream start codon. LMJ-040682 was transformed with both pAS_C2 and pAS_C3, and
298 representative transformant lines selected via antibiotic resistance were obtained. These, together with
299 their parental strains were grown in the presence or absence of 10 µM thiamine for 5 days, and then
300 used in the B₁₂ uptake assay. Transformants of both LMJ-040682::pAS_C2 and LMJ-
301 040682::pAS_C3 were found to take up B₁₂ to a similar extent as their parental strain cw15 when
302 grown in the absence of thiamine (Figure 4b). However, when 10 µM thiamine was included in the
303 culture medium, LMJ-040682::pAS_C3 showed virtually no B₁₂ uptake. This riboswitch-mediated
304 conditional complementation of the phenotype in LMJ-040682::pAS_C3 demonstrated conclusively
305 that B₁₂ uptake in *C. reinhardtii* is dependent on the presence of CrCBA1.

306

307
308
309
310
311
312
313
314
315
316
317
318
319
320
321
322
323
324
325
326
327
328
329
330
331
332
333
334

CrCBA1 shows an association with membranes and is highly upregulated under B₁₂-deprivation

To investigate the subcellular location of CrCBA1, we used several bioinformatic targeting prediction tools. CrCBA1 is annotated as a flagella-associated protein in the Phytozome v5.6 *C. reinhardtii* annotation. However, both DeepLoc (Almagro Armenteros et al., 2017) and SignalP (Almagro Armenteros et al., 2019), as well as AlphaFold2, indicated a hydrophobic sequence with the characteristics of a signal peptide at the N-terminus of CrCBA1 and predicted it would be targeted to the endoplasmic reticulum (ER). Additionally, it was predicted to contain a transmembrane helix at its C-terminus by InterPro (Mitchell et al., 2019) and AlphaFold2.

We next investigated the subcellular location of CrCBA1 *in vivo* by imaging two lines of LMJ-040682::pAS_C2, where the CBA1 is tagged with mVenus, with confocal microscopy. No mVenus was detected in the parental LMJ-040682 cells, whereas a clear fluorescent signal was observed in LMJ-040682::pAS_C2 #A10 and LMJ-040682::pAS_C2 #D10 (Figure 5). In these complemented lines, the mVenus signal was absent from the chloroplast, nucleus and flagella, but instead could be seen within the cell localising both to the plasma membrane and to regions that may be endomembranes such as the ER. This is consistent with findings from *P. tricornutum* showing a similar distribution (Bertrand et al., 2012). Together these data indicate that CBA1 is likely to be associated with membranes, and therefore, may have a conserved role in the B₁₂ uptake process.

Further evidence for the role of CBA1 in B₁₂ uptake was obtained by taking advantage of a B₁₂-dependent mutant of *C. reinhardtii*, metE7 (Helliwell et al., 2015; Bunbury et al., 2020). We tested the effect of B₁₂-deprivation over time on the expression of the *CrCBA1* gene by RT-qPCR in the mutant and determined the rate of B₁₂ uptake over a similar period. Within 6h of B₁₂ removal, there was a ~250-fold induction of the *CrCBA1* transcript, followed by a slow decline over the next 60h (Figure 6a). After resupply of B₁₂ there was then a rapid ~100-fold decline within 8h. The B₁₂ uptake capacity of metE7 followed a similar profile, increasing 3-fold over the first 12 hours of B₁₂ depletion,

335 from $\sim 6.5 \times 10^5$ molecules B_{12} /cell/hour to 1.86×10^6 molecules B_{12} /cell/hour (Figure 6b), then
336 declining slowly. This induction profile is characteristic of a nutrient-starvation response shown by
337 many transporters, including in *C. reinhardtii* those for Fe (Allen et al., 2007), and for *CBA1* in the
338 B_{12} -dependent diatom, *Thalassiosira pseudonana* (Bertrand et al., 2012).

339

340 **Widespread distribution of CBA1 in algae**

341 Having shown the importance of *PtCBA1* and *CrCBA1* for B_{12} uptake in their respective species, we
342 re-examined how prevalent CBA1-like proteins are in Nature. Searches with BLASTP using *PtCBA1*
343 were reported to result in no significant hits in species outside the Stramenopiles (Bertrand et al.,
344 2012). Instead, we created a hidden Markov model (HMM), using the *C. reinhardtii* CBA1 amino
345 acid sequence and CBA1 sequences from *P. tricornutum*, *T. pseudonana*, *Fragilariopsis cylindrus*,
346 *Aureococcus anophagefferens* and *Ectocarpus siliculosus* (Bertrand et al., 2012), to identify more
347 accurately CBA1-like proteins in other organisms. The EukProt database of curated eukaryotic
348 genomes (Richter et al. 2022) includes representatives from the Archaeplastida (designated by
349 EukProt as Chloroplastida), which encompass green algae, red algae, glaucophytes and all land plants,
350 as well as phyla that include algae with complex plastids, namely Stramenopiles (which include
351 diatoms), Alveolata (including dinoflagellates), Rhizaria and Haptophyta, and the animals (both
352 Metazoa and the Choanoflagellates, the closest living relatives of the animals), the fungi and
353 Amoebozoa. This database was queried with the CBA1 HMM model, using a cutoff e-value of $1e-20$,
354 and 277 hits were obtained (Supplemental Figure S7; Supplemental Table S4). No candidates were
355 found in the Metazoa, but CBA1 homologues were identified in all other phyla, including all
356 photosynthetic groups, fungi and amoebozoa and in choanoflagellates, unicellular and colonial
357 flagellated organisms considered to be the closest living relatives of animals (King et al., 2008).

358

359 Given that vascular plants have no B_{12} -dependent enzymes, the presence of a putative B_{12} -binding
360 protein in several angiosperms, both monocot and dicot, and the gymnosperm *Ginkgo biloba*, was
361 somewhat surprising. To address this conundrum, we investigated to what extent CBA1 was
362 associated with vitamin B_{12} dependence by determining the distribution of the different isoforms of

363 methionine synthase, METH and METE. Using the same HMM approach as before, the protein
364 sequences were searched against the EukProt database and the combination of presence and absence
365 of CBA1, METH and METE across eukaryotic species groups was compiled (Figure 7; Supplemental
366 Table S5). What is immediately apparent is that the combination of the three proteins is quite different
367 in the various lineages. In the major algal groups, the Chlorophyta and the SAR clade (Stramenopiles,
368 Alveolata and Rhizaria), METH sequences were found in the majority of genomes analysed and their
369 presence was associated with CBA1. In the genomes of the Chlorophyta and the SAR clade that
370 encoded METE only (7 taxa in total), CBA1 was absent in all but one, the diatom *Thalassionema*
371 *nitzschoides*. Equal numbers of Alveolata species encoded METH and CBA1, or METH only;
372 interestingly, the latter were all non-photosynthetic lineages. Grouping the data from these 4 algal
373 groups, a Chi Square test was significant for CBA1 and METH being more often both present or both
374 absent ($\chi^2(1, N = 86) = 9.2, p = 0.00240$). The association could be due to linkage, although in
375 neither *C. reinhardtii* nor *P. tricornutum* are the two genes on the same chromosome, making this
376 unlikely. Alternatively, there is a fitness advantage in both genes being acquired or lost together.
377
378 Most fungal taxa lacked both METH and CBA1, but we found examples of 6 species that were
379 predicted to be B₁₂ users (METH present) and 5 of these were also predicted to contain CBA1-like
380 sequences: *Allomyces macrogynus*, *Spizellomyces punctatus*, *Rhizophagus irregularis*, *Rhizopus*
381 *delemar* and *Phycomyces blakesleeanus*. CBA1-like sequences were identified in the Opisthokonta
382 and Amoebozoa, although were less prevalent, with ~23% of choanoflagellates and 8% of amoeboid
383 species being like algae in having both METH and CBA1. CBA1 was entirely absent from the
384 Metazoa. In contrast, in the Streptophyta, which include multicellular green algae and all land plants,
385 the majority lack METH, but almost 80% of species were found to contain CBA1-like sequences.
386 This implies that Streptophyta CBA1 sequences may have gained a different function, which would
387 be consistent with the lack of B₁₂-dependent metabolism in these organisms. In summary, these data
388 suggest that CBA1 is associated with vitamin B₁₂ use to different degrees in different eukaryotic
389 groups, with there being a greater association in obligate and facultative B₁₂ users than in those
390 organisms that do not utilise B₁₂.

391
392
393
394
395
396
397
398
399
400
401
402
403
404
405
406
407
408
409
410
411
412
413
414
415
416
417
418

The many putative CBA1 homologues in algal lineages and their strong association with B₁₂ uptake provided an opportunity to identify conserved, and thus likely functionally important, residues. Accordingly, a multiple sequence alignment of proteins matching the CBA1 HMM query was generated (Supplemental Figure S7). Highlighted in green in the similarity matrix at the top are nine conserved regions with several almost completely conserved residues; these are shown in more detail in Figure 8a for selected taxa representing different algal groups. Further insight came from inspection of the model of the 3D structure of CrCBA1 generated by the AlphaFold2 protein structure database. The analysis showed that regions of CrCBA1 showed similarity to bacterial periplasmic binding proteins, including the B₁₂-binding protein BtuF. A structure is available of *E. coli* BtuF in complex with B₁₂ (Borths et al., 2002), so we compared this to the modelled CrCBA1 structure. Although there is little sequence similarity, alignment of the two structures resulted in an RMSD of 3.362 and enabled the relative position of B₁₂ to be placed in the lower cleft of CrCBA1, shown in red in Figure 8b. Mapping of the highly conserved residues onto this structure found that four (W255, W394, F395 and E396) were in a cluster around the relative position of B₁₂. Another cluster of highly conserved residues were located at the end of the upper alpha helix (K78, P118, L136, F214, F215, N216 and E218). Both clusters represent promising mutational targets to investigate CrCBA1 function.

DISCUSSION

In this study we have shown experimentally that a conserved protein, CBA1, is required for the uptake of the micronutrient B₁₂ in two taxonomically distant algae, the diatom *P. tricornutum* (Figure 1) and the chlorophyte *C. reinhardtii* (Figures 3 & 4). Strains with knockouts of the gene were unable to take up B₁₂, demonstrating that there is no functional redundancy of this protein in either organism. As well as providing evidence that CBA1 is present outside the Stramenopiles, we found widespread occurrence of CBA1 homologues with considerable sequence conservation across eukaryotic lineages (Figures 7 and Supplemental S7). The strong association of CBA1 with the B₁₂-dependent methionine synthase, METH, in algal lineages, provides evidence that CBA1 is a key component of the B₁₂

419 uptake process in evolutionarily distinct microalgae, and the structural similarities between CBA1 and
420 BtuF (Figure 8b) suggest it may operate as a B₁₂-binding protein. The highly conserved residues
421 identified in the algal homologues (Figure 8a) offer the means to establish which are functionally
422 important, facilitated by the uptake assay we established.

423

424 Nonetheless, the mechanistic role of CBA1 in the process of B₁₂ acquisition in algae is not yet clear.
425 Previous physiological studies of B₁₂ uptake by microalgae, such as the haptophyte *Diacronema*
426 *lutheri* (Droop, 1968), indicated a biphasic process: firstly rapid irreversible adsorption of B₁₂ to the
427 cell exterior, followed by a slower second step of B₁₂ uptake into the cell, consistent with endocytosis.
428 CBA1 is unlikely to be associated with the binding of B₁₂ in the cell wall, however. This is because
429 the *C. reinhardtii* strains used in this study, UVM4 and CW15, were cell wall deficient, and therefore
430 likely also deficient in cell wall proteins that bind B₁₂; the lack of a B₁₂-BODIPY signal from the cell
431 surface in IM4 (Supplemental Figure S2) supports this hypothesis. Further use of this fluorescent
432 probe offers the possibility to monitor the localisation of B₁₂-BODIPIY over time to gain insights into
433 the stages of B₁₂ uptake, as has been done in other organisms (Lawrence et al., 2018). In addition,
434 confocal microscopy of CBA1-mVenus fusion protein in *C. reinhardtii* (Figure 5) showed an apparent
435 association of CrCBA1 with the plasma membrane and endomembranes, which is similar to that for
436 ER-localised proteins (Mackinder et al., 2017). Moreover, in a proteomics study of lipid droplets
437 (which form by budding from the ER) CBA1 was in the top 20 most abundant proteins (Goold et al.,
438 2016). Bertrand et al. (2012) found that PtCBA1 had a signal peptide and fluorescently tagged
439 PtCBA1 was also targeted to the ER. Nonetheless, based on its predicted 3D structure and the fact that
440 it has at most one transmembrane helix, CBA1 does not appear to be a transporter itself. Instead,
441 given its structural similarity to BtuF, a distinct possibility is that CBA1 is the soluble component of
442 an ABC transporter, either at the plasma membrane or an internal membrane, and likely will interact
443 with one or more other proteins to allow B₁₂ uptake to occur, at least some of them being those
444 involved in receptor-mediated endocytosis, as is the case for B₁₂ acquisition in humans (Rutsch et al.,
445 2009; Beedholm-Ebsen et al., 2010; Coelho et al., 2012). In this context, there are known similarities
446 between endocytosis in *C. reinhardtii* and humans (Denning and Fulton, 1989; Bykov et al., 2017),

447 and several putative homologues have been identified by sequence similarity in the alga. Testing the
448 B₁₂-uptake capacity of mutants of these proteins would be one approach to investigate whether their
449 roles are also conserved.

450

451 In contrast to the situation in algae, the Streptophyta live in a B₁₂-free world, neither synthesising nor
452 utilising this cofactor. This is exemplified by the fact that in our analysis only one species, the
453 charophyte alga *Cylindrocystis brebissonii*, encoded METH. Despite this, more than three-quarters of
454 this group encode a CBA1 homologue (Figures 7 & S7). Since the majority of the conserved residues
455 (Figure 8a) are also found in putative CBA1 sequences in the angiosperms such as *Arabidopsis*,
456 including those around the potential binding pocket, it is possible that the streptophyte protein has
457 acquired a new function that still binds a tetrapyrrole molecule. Intriguingly, the reverse is observed in
458 the Metazoa, where METH is almost universal, but CBA1 is entirely absent. However, some
459 Choanoflagellates and some species of fungi do appear to encode both METH and CBA1, suggesting
460 that they utilise B₁₂, a trait recognised to occur in fungi only recently (Orłowska et al., 2021). It will
461 be of interest therefore to test whether CBA1 is involved in B₁₂ uptake in these organisms, for
462 example by gene knockout studies.

463

464 The importance of B₁₂ availability for phytoplankton productivity has been demonstrated across
465 several marine ecosystems by amendment experiments (e.g. Bertrand et al., 2011; Koch et al., 2012;
466 Joglar et al., 2021), where addition of B₁₂ led to algal blooms and affected the composition and
467 stability of microbial communities. The mode of acquisition of this micronutrient is thus likely to be
468 highly conserved and subject to substantial ecological and evolutionary selection pressure to be
469 retained. Moreover, the role of B₁₂ at the cellular level may well provide a direct connection between
470 environmental conditions and the epigenetic status of the genome: methionine synthase is the key
471 enzyme in C1 metabolism, linking the folate and methylation cycles and thus responsible for
472 maintaining levels of S-adenosylmethionine (SAM) the universal methyl donor (Hanson & Roje
473 2001; Mentch & Locasale, 2016). In this context, it is noteworthy that the knockout of *CBA1* in the
474 IM4 line was the result of insertion of a class II transposable element into the gene. This mobilization

475 is likely to reflect epigenetic alterations of the autonomous element, presumably as a result of cellular
476 stress either from the antibiotic selection, or the transformation procedure, or both. Recent
477 classification of the transposons in *C. reinhardtii* indicate that the transposon inserted into *CBA1* in
478 IM4 is a member of the KDZ superfamily of class II TIR elements named Kyakuja-3_cRei (Craig et
479 al. 2021). If the phenomenon of inactivation of a gene that is deleterious (in this case allowing B₁₂ to
480 be taken up and repress the antibiotic resistance gene) via transposition is a general response in *C.*
481 *reinhardtii*, repeating the screen for CBA1 mutants might allow observation of further transposition
482 events, and enable characterisation of this group of elements at the functional level. Moreover, it
483 could be adopted as a more general methodology to identify candidate genes involved in other
484 physiological processes, by tying their expected effects to deleterious outcomes through synthetic
485 biology constructs and screening surviving mutants by sequencing.

486

487

488 **MATERIALS AND METHODS**

489

490 **Organisms and growth conditions**

491 Strains, media and growth conditions used in this study are listed in Table S1. If required, antibiotics,
492 vitamin B₁₂ (cyanocobalamin) and thiamine were added to the medium at concentrations indicated.
493 Algal culture density was measured using a Z2 particle count analyser (Beckman Coulter Ltd.) and
494 optical density (OD) at 730 nm was measured using a FluoStar OPTIMA (BMG labtech) plate reader
495 or a CLARIOstar plate reader (BMG labtech). Bacterial growth was recorded by measuring OD₅₉₅.

496

497 **Algal B₁₂-uptake assay**

498 Algal cultures were grown to stationary phase and cyanocobalamin salt (Sigma) was added
499 (*Phaeodactylum tricornerutum*: 600 pg; *Chlamydomonas reinhardtii*: 150 pg) to 5 x 10⁶ cells in a final
500 volume of 1 ml in f/2 or TAP medium respectively. The samples were incubated at 25°C under
501 continuous light with shaking for 1 hour and inverted every 30 minutes to aid mixing. Samples were
502 centrifuged and the supernatant (media fraction) transferred into a fresh microcentrifuge tube. The cell

503 pellet was resuspended in 1 ml water. Both samples were boiled for 10-20 minutes to release any
504 cellular or bound B₁₂ into solution, and then centrifuged to pellet debris. The supernatant was used in
505 the *S. typhimurium* B₁₂ bioassay as described in Bunbury et al. (2020). The amount of B₁₂ in the
506 sample was calculated by comparison to a standard curve of known B₁₂ concentrations fitted to a 4
507 parameter logistic equation $f(x) = c + (d-c)(1+\exp(b(\log(x)-\log(e))))$ (Ritz et al., 2015). This standard
508 curve was regenerated with every bioassay experiment.

509

510 **Generating *P. tricornutum* CBA1 knockout lines using CRISPR-Cas9**

511 CRISPR/Cas9 genome editing applied the single guide RNA (sgRNA) design strategy described in
512 Hopes et al., (2017). Details are provided in the Supplemental methods. *P. tricornutum* CCAP 1055/1
513 cells were co-transformed with linearised plasmids pMLP2117 and pMLP2127 (Supplemental Table
514 2) using a NEPA21 Type II electroporator (Nepa Gene) as previously described (Yu et al., 2021).
515 After plating on 1% agar selection plates containing 75 mg·l⁻¹ zeocin and incubation for 2-3 weeks,
516 zeocin resistant colonies were picked into 96 well plates containing 200 µl of f/2 media with 75 mg·l⁻¹
517 zeocin. After seven days strains were subcultured into fresh media either containing 75 mg·l⁻¹ zeocin
518 or 300 mg·l⁻¹ nourseothricin, and genotyped with a three-primer PCR using PHIRE polymerase
519 (Thermo Fisher Scientific) with primers gCBA1.fwd, gCBA1.rv and NAT.rv (Supplemental Table
520 S3). Five promising colonies resistant to nourseothricin and with genotypes showing homologous
521 recombination or indels were re-streaked on 75 mg·l⁻¹ zeocin f/2 plates to obtain secondary
522 monoclonal colonies. Twelve secondary colonies were picked for each primary colony after 2-3
523 weeks and again genotyped with a three-primer PCR. Promising colonies were genotyped in further
524 detail with primer pairs gCBA1.fwd/gCBA1.rv, gCBA1.fwd/NAT.rv and gCBA1in.fwd/gCBA1in.rv
525 (Supplemental Table S3).

526

527 **Construct assembly and *C. reinhardtii* transformation**

528 Constructs were generated using Golden Gate cloning, using parts from the *Chlamydomonas* MoClo
529 toolkit (Crozet et al., 2018) and some that were created in this work. All parts relating to
530 *Cre02.g081050* were domesticated from UVM4 genomic DNA, with BpiI and BsaI sites removed

531 from the promoter, ORF and terminator by PCR-based mutagenesis using primers listed in
532 Supplemental Table S3. A list of plasmids used in this study is shown in Supplemental Table S2.
533 Transformation of *C. reinhardtii* cultures with linearised DNA was carried out by electroporation
534 essentially as described by Mehrshahi et al. (2020) before plating on TAP-agar plates with the
535 appropriate antibiotics.

536
537 Insertional mutagenesis was performed as above, however, cultures were grown to a density of
538 approximately 1×10^7 cells/ml and were incubated with 500 ng transgene cassette. After allowing the
539 cells to recover overnight in TAP plus 60 mM sucrose at 25°C in low light (less than 10 $\mu\text{mol photon}$
540 $\text{m}^{-2} \cdot \text{s}^{-1}$ at 100 rpm), between 200 - 250 μl of transformants were plated on solid TAP media (square
541 12x12 cm petri dishes) containing ranges of 15-20 $\mu\text{g/ml}$ hygromycin, 20-50 $\mu\text{g/ml}$ paromomycin and
542 48-1024 ng/l vitamin B12, and the plates were incubated in standing incubators.

543 544 **Confocal laser scanning microscopy**

545 *C. reinhardtii* transformants carrying the pAS_C2 construct were imaged in a confocal laser scanning
546 microscope (TCS SP8, Leica Microsystems, Germany) with an HC PL APO CS2 40x/1.30 aperture
547 oil-immersion lens. Images were taken using the sequential mode provided by the Leica LAS
548 software, with the channel used for mVenus and brightfield detection being taken first and the channel
549 used for chlorophyll detection taken second. The first image was acquired with excitation from a
550 white light source at 486 nm at 7% power and emissions were detected between 520 - 567 nm;
551 mVenus settings included 100% gain, gating between 0-8.24 ns and a reference line at 486 nm.
552 Brightfield imaging used 610% gain and a 0% offset. Frames were captured with a line average of 4
553 and a frame accumulation of 2. The second image was acquired with excitation from a white light
554 source at 514 nm at 2% power and emissions were detected between 687 - 724 nm with 50% gain.
555 Frames were captured with a line average of 4 and a frame accumulation of 1. The overlay images
556 were produced automatically by the Leica LAS software. Inkscape was used to increase the lightness
557 and decrease the contrast of all the images in the same manner.

558

559 **Reverse transcription quantitative PCR**

560 Quantification of steady state levels of transcripts was carried out according to Bunbury et al. (2020),
561 using random hexamer primers for cDNA synthesis. The RT-qPCR data was analysed using the
562 $\Delta\Delta\text{CT}$ method with an assumed amplification efficiency of 2. $\text{Log}_2(2^{-\Delta\text{CT}})$ values were plotted in the
563 resulting figures.

564 **Whole genome sequencing**

565 Genomic DNA was extracted from *C. reinhardtii* cells by phenol-chloroform extraction and
566 sequenced using the NovaSeq sequencing platform by Novogene (Cambridge, UK) to produce 150 bp
567 paired-end reads. This involved RNase treatment and library preparation with the NEBNext Ultra II
568 DNA Library Prep Kit (PCR-free), which generated 350 bp inserts. The raw sequencing data for this
569 study have been deposited in the European Nucleotide Archive (ENA) at EMBL-EBI under accession
570 number PRJEB58730 (<https://www.ebi.ac.uk/ena/browser/view/PRJEB58730>). Novogene performed
571 all quality filtering, summary statistics and bioinformatic analysis. The location of the Hyg3 cassette
572 was determined by identifying loci that comprised reads from IM4 that mapped between genomic
573 DNA and pHyg3, and cross-referencing these loci against the parental strains. The TE identification
574 was carried out similarly, full details are provided in Supplemental Methods.

575 **Bioinformatics pipeline**

576 The EukProt database was assessed for the presence of METE, METH and CBA1 (Richter et al.,
577 2022). The query used for CBA1 was a hidden Markov model (HMM) generated from the protein
578 fasta sequences: Phatr3_J48322, Thaps3 11697, Fracy1 241429, Fracy1 246327, Auran1 63075,
579 *Ectocarpus siliculosus* D8LMT1 and Cre02.g081050.t1.2 by first aligning using MAFFT (Kato and
580 Standley, 2013) version 7.470 with the --auto option, and then building a HMM using hmmbuild
581 (hmmer 3.2.1). Additionally, protein fasta (Cre06.g250902, Cre03.g180750), PFAM (PF02310,
582 PF02965, PF00809, PF02574, PF01717, PF08267) and KO (K00548, K00549) queries were searched
583 against EukProt to identify sequences with similarity to METE and METH. The queries were
584 searched against EukProt using hmmsearch (HMMER 3.1b2). The default bitscore thresholds were
585
586

587 used for KO and PFAM queries. The threshold used for CBA1 HMM, and the CrMETE and CrMETH
588 protein fasta sequences, was a full-length e-value of 1e-20. For each protein, all individual queries
589 were required to be significant to classify the protein as present. The best hit in each species was
590 identified by taking the protein with the greatest geometric mean of full length bitscores for the
591 queries. The dataset was joined with taxonomic information from EukProt and completeness
592 information calculated using BUSCO version 4.1.4 and eukaryote_odb10 (Manni et al., 2021).

593

594 **Accession Numbers**

595 Sequence data from this article can be found in the GenBank/EMBL data libraries under
596 accession numbers_ PRJEB58730 (<https://www.ebi.ac.uk/ena/browser/view/PRJEB58730>).

597

598 **Supplemental Data**

599

600 Supplemental Figure S1. Characterization of B₁₂ uptake in *C. reinhardtii* insertional mutant
601 lines.

602 Supplemental Figure S2. Visualization of B₁₂-BODIPY uptake in *C. reinhardtii* using confocal
603 microscopy

604 Supplemental Figure S3. *C. reinhardtii* knockout lines of *Cre12.g508644* are able to take up B₁₂

605 Supplemental Figure S4. Structure and sequence of a second insertion in the IM4 strain

606 Supplemental Figure S5. The predicted structures of CrCBA1 and PtCBA1 show a high degree of
607 structural similarity.

608 Supplemental Figure S6. Independent mutant lines of *CrCBA1* show defective B₁₂ uptake

609 Supplemental Figure S7. Sequences with similarity to CBA1 are found throughout Eukaryota

610 Supplemental Table S1. Table of strains used in this work

611 Supplemental Table S2. Plasmids used in this study

612 Supplemental Table S3. Oligonucleotides used in this study

613 Supplemental Table S4. Protein sequences with similarity to CBA1 used for tree building in Figure
614 S7.

615 Supplemental Table S5. Summary of CBA1, METE and METH presence/absence found in
616 organisms within Supergroups with greater than 5 organisms with a completeness greater than 70%
617 and at least one of: METE or METH.

618 Supplemental Methods

619

620

621 **Funding information**

622 This work was supported by the UK's Biotechnology and Biological Sciences Research Council
623 (BBSRC) Doctoral Training Partnership, grant no. BB/M011194/1 to A.P.S., M.L.P. and A.G.S; grant
624 no. BB/M018180/ 1 to P.M. and A.G.S.; grant no. BB/L002957/1 and BB/R021694/1 to K.G. and
625 AGS; grant no. BB/L014130/1 to G.I.M, K.G., P.M. and A.G.S; grant no. BB/S002197/1 to M.J.W;
626 University of Cambridge Broodbank Fellowship to G.I.M; Royal Society grant no. INF\R2\180062 to
627 M.J.W.; and Bill & Melinda Gates Foundation OPP1144 and Gates Cambridge Trust (Graduate
628 Student Fellowship) to A.H.

629

630 **Acknowledgements**

631 We thank Catherine Sutherland for help with maintaining and screening the CRISPR/Cas9 mutants of *P.*
632 *tricornutum* and Dr Lorraine Archer for lab management. We are grateful to Dr Amanda Hopes and Prof
633 Thomas Mock (University of East Anglia) for the parts used in gene editing of *PtCBA1*. The plasmid Hyg3
634 used in the insertional mutagenesis was obtained from the Chlamydomonas Resource Centre
635 (www.chlamycollection.org). For the purpose of open access, the authors have applied a Creative Commons
636 Attribution (CC BY) licence to any Author Accepted Manuscript version arising from this submission.

637

638

639

640 **Author contributions**

641 APS designed and performed research, analysed data and wrote the article with contributions from all
 642 the authors. KG and MLP carried out the CRISPR/Cas9 editing of *P. tricornutum* and contributed to
 643 writing the article. AH carried out the bioinformatics analysis to identify the putative transposable
 644 elements. FB performed the *metE7* RT-qPCR and B₁₂ uptake assays. MJW & ADL synthesised the
 645 BODIPY-labelled B₁₂ and contributed to writing the article. KG, GMO and PM supervised aspects of
 646 the project and contributed to writing the article. AGS conceived the project, obtained the funding,
 647 supervised the project and wrote the article with contributions from all the authors. AGS agrees to
 648 serve as the author responsible for contact and ensures communication.

649

650

651 **Figure Legends**

652

653 **Figure 1. Disruption of *Phaeodactylum tricornutum* CBA1 (*PtCBA1*) using CRISPR-**
 654 **Cas9 yielded lines with impaired B₁₂ uptake. a)** Schematic showing CRISPR-Cas9 sgRNA
 655 target sites and the homology repair template design used to generate mutant lines in *PtCBA1*
 656 (Phatr3_J48322). The homology repair template schematic is annotated with the 5' homology
 657 region (HR) and 3'HR, the *FCPB* promoter, nourseothricin resistance gene (*NAT*) and *FCPC*
 658 terminator. The *PtCBA1* gene is annotated with the ORF, the 5'HR and 3'HR regions used in
 659 the homology template and the regions of the ORF targeted by sgRNA (vertical bars). Primer
 660 positions used for the analysis of putative mutant lines are shown with arrowheads. **b)** PCR of
 661 regions across and within wild-type (WT) and mutant *PtCBA1* in 3 independent CRISPR-
 662 Cas9 lines (Δ CBA1) showing indel mutations in the mutants. PCR products from different
 663 sets of primers indicated in panel a are shown. M = marker, - Ctrl = no DNA template. **c)** A
 664 B₁₂ uptake assay was performed as described in Materials and Methods, to determine the
 665 amount of B₁₂ in the media and the cells after 1h incubation of *P. tricornutum* cells in 600 pg
 666 B₁₂. The 'Total' was inferred by the addition of the cell and media fractions. The dashed line
 667 indicates the amount of B₁₂ added to the experiment. Standard deviation error bars are shown,
 668 n=4. Statistical analysis was performed on the media fraction, and Tukey's test identified the
 669 following comparisons to be significantly different from one another: WT vs No Algae
 670 ($p < 1e^{-12}$); WT vs Δ CBA1-1 ($p < 1e^{-10}$); WT vs Δ CBA1-2 ($p < 1e^{-12}$); WT vs Δ CBA1-3 ($p < 1e^{-$
 671 11); No Algae vs Δ CBA1-1 ($p < 1e^{-03}$); No Algae vs Δ CBA1-3 ($p < 0.05$); and Δ CBA1-1 vs
 672 Δ CBA1-2 ($p < 1e^{-02}$).

673

674

675 **Figure 2. Generation and use of *C. reinhardtii* reporter strain UVM4-T12 for insertional**
 676 **mutagenesis. a)** Schematic of the constructs used for insertional mutagenesis of *C.*

677 *reinhardtii*. The pAS_R1 construct was designed to control expression of the paromomycin
 678 resistance gene (*aphVIII*) via B₁₂ mediated repression of the *METE* promoter (*P_{METE}*). The
 679 pHyg3 construct encoded a constitutively expressed hygromycin resistance gene (*aphVII*), to
 680 be used for insertional mutagenesis. **b)** Growth of *C. reinhardtii* B₁₂ reporter strain UVM4-

681 T12 bearing pAS_R1 plasmid, in response to vitamin B₁₂ and paromomycin concentration in
682 the media according to the algal dose-response assay. The predicted dose-response model is
683 shown in black, with 95% confidence intervals in grey.
684
685

686 **Figure 3. *C. reinhardtii* insertional mutant 4 (IM4) is defective in B₁₂ response and**
687 **uptake, and can be functionally complemented with *CrCBA1*.** a) Effect of vitamin B₁₂ on
688 *METE* gene expression in UVM4 and IM4, determined by RT-qPCR. UVM4 and IM4 were
689 grown in TAP media with or without 1000 ng·l⁻¹ vitamin B₁₂ for 4 days at 25°C, 120 rpm and
690 in continuous light (90 μE·m⁻²·s⁻¹). Boxplots of the log₂ transformed expression level of
691 *METE* relative to that in the control (no B₁₂) sample are shown, n=6. The boxplots show the
692 median (center line), 25th and 75th percentile hinges, and whiskers extending to the value no
693 further than 1.5 times the interquartile range; values beyond this are plotted
694 individually. Significant comparisons were identified using Tukey's test: UVM4 + 1000 ng·l⁻¹
695 vitamin B₁₂ from UVM4 No Addition (p<1e⁻⁰⁸), IM4 No Addition (p<1e⁻⁰⁸) and IM4 +
696 1000 ng·l⁻¹ vitamin B₁₂ (p<1e⁻⁰⁷). b) Schematic of the Cre02.g081050 gene showing the
697 position of the insertion site (indicated with a black triangle) determined by whole genome
698 sequencing (Figure S4). c) Schematic of the pAS_C2 construct designed to express *CrCBA1*
699 fused to the fluorescent reporter mVenus. *CrCBA1-mVenus* was under the control of the
700 *CrCBA1* promoter and terminator. pAS_C2 also contained the spectinomycin resistance gene
701 *aadA*, driven by the *PSAD* promoter and *PSAD* terminator. d) B₁₂-uptake assay with UVM4,
702 IM4 and IM4::pAS_C2 (n =4 separate transformants with high mVenus expression). Dashed
703 line indicates the amount of B₁₂ added to the assay. Standard deviation error bars are shown.
704 Statistical analysis was performed on the media fraction, and Tukey's test identified the
705 following comparisons to be significantly different from one another: No Algae vs UVM4
706 (p<1e⁻⁰⁵); No Algae vs IM4 (p<0.05); No Algae vs IM4::pAS_C2 (p<1e⁻⁰³); UVM4 vs 1.G2
707 (p<1e⁻⁰⁹); and 1.G2 vs 1.G2::pAS_C2 (p<1e⁻⁰⁶).
708
709

710 **Figure 4. CLiP mutants in *CrCBA1* are impaired in their ability to take up B₁₂.** a)
711 Schematic of the pAS_C3 construct designed to express *CrCBA1* in a controllable manner
712 using a thiamine repressible riboswitch (RS_{THI4_4N}) to allow repression of *CrCBA1* through
713 the addition of thiamine (Mehrshahi et al., 2020). b) B₁₂-uptake assay with cw15, LMJ-
714 040682 (mean of 4 independent transformants) and LMJ-040682::pAS_C2 and LMJ-
715 040682::pAS_C3 (mean of 3 independent transformants). The growth conditions were
716 modified compared to previous assays: lines were grown with or without 10 μM thiamine
717 supplementation for 5 days in a 16/8 light/dark cycle, and 8 hours after the dark to light
718 transition the cultures were used for the algal B₁₂-uptake assay. The dashed line indicates the
719 amount of B₁₂ added to the sample. Standard deviation error bars are shown. Statistical
720 analysis was performed on the media fraction. Tukey's test identified the following algal
721 strains to be significantly different from one another in media without thiamine (not reporting
722 comparisons against the No Algae control condition): cw15 vs LMJ-040682 (p<1e⁻¹⁰); LMJ-
723 040682 vs LMJ-040682::pAS_C2 (p<1e⁻⁰⁹); and LMJ-040682 vs LMJ-040682::pAS_C3
724 (p<1e⁻⁰⁹). Additionally, Tukey's test found the following strain to show a significant
725 difference due to thiamine addition: LMJ-040682::pAS_C3 (p<1e⁻⁰⁷).
726
727

728 **Figure 5. Confocal microscopy of complemented *C. reinhardtii* *CrCBA1* knockout lines**
729 **showing an association between *CrCBA1* and membranes.** LMJ-040682 and LMJ-
730 040682::pAS_C2 A10 and D10 lines were imaged according to the protocol outlined in the

731 materials and methods. Channels shown (left to right) are brightfield, chlorophyll, mVenus
732 and an overlay. Microscope settings are described in Methods.

733

734 **Figure 6. CBA1 expression and B₁₂ uptake capacity in a B₁₂-dependent mutant of *C.***
735 ***reinhardtii* (metE7) during B₁₂ starvation and add-back.** a) Log₂ transformed expression
736 level of CBA1 measured by RT-qPCR and presented relative to levels in control conditions
737 (B₁₂ replete). Vertical dashed lines denote when B₁₂ was removed and added. b) B₁₂ uptake
738 capacity of starved metE7 cells (expressed as 10⁶ molecules of B₁₂ per cell over 1h) at the
739 same 6 time points during B₁₂ starvation; it was not possible to perform the uptake assay on
740 cells to which B₁₂ had already been added. Cell density measurements were performed by
741 counting plated cells in dilution series, and so included non-viable cells. For CBA1
742 expression and B₁₂ uptake, 3 and 6 biological replicates were used, respectively, with points
743 representing means, and error bars representing standard deviations.

744

745

746 **Figure 7. Distribution of CBA1 and methionine synthase sequences across Eukaryotic**
747 **groups.** The EukProt database (Richter et al., 2022) was searched for METE, METH and
748 CBA1 queries, as described in the materials and methods. Organisms were only considered if
749 they contained at least one valid methionine synthase hit (METE or METH) and their
750 genomes were >70% complete, as measured by BUSCO (Manni et al., 2021). Eukaryotic
751 classes were filtered for those with greater than 5 genomes and the numbers of taxa for each
752 class are indicated in brackets. The different combinations of CBA1, METE and METH were
753 calculated for each species (Supplemental Table S4) and summarised as a percentage of the
754 total number of taxa in each class, with gradual shading to show the variation in distribution
755 between the different classes.

756

757

758 **Figure 8. Identification and predicted structural location of CrCBA1 conserved**
759 **residues.** a) Sequences with similarity to CBA1 were identified from the EukProt database
760 (Richter et al., 2022) using a manually generated CBA1 Hidden Markov Model (HMM), as
761 described in the materials and methods. A selection of 16 taxa from several eukaryotic
762 supergroups were chosen and conserved regions from the protein are presented. Specific
763 residues indicated by * are: K78, P118, L136, E206, F214, F215, N216, E218, P251, V253,
764 W255, G289, W394, F395, E396 and D408. Protein sequences are coloured according to the
765 Clustal colour-scheme using Geneious Prime 2021.1.1 (www.geneious.com). For each highly
766 conserved region, the corresponding position and amino acid from the CrCBA1 sequence
767 (Cre02.g081050) is indicated. b) The predicted 3D structure of CrCBA1 (residues 21-490)
768 was obtained from the AlphaFold Protein Structure Database (entry: A0A2K3E0J7). Highly
769 conserved regions of CrCBA1 are indicated in light blue and labelled. CrCBA1 was aligned
770 to the crystal structure of *E. coli* BtuF in complex with B12 (pdb: 1n2z). This enabled the
771 relative position of B12 (shown in red) to be superimposed onto CrCBA1.

772

773

774

775

776 **References**

777

778 **Allen, MD, del Campo JA, Kropat J, Merchant SS (2007) FEA1, FEA2, and FRE1, encoding**
779 **two homologous secreted proteins and a candidate ferrireductase, are expressed coordinately with**
780 **FOX1 and FTR1 in iron-deficient *Chlamydomonas reinhardtii*.** *Eukaryotic Cell* **6**: 1841–1852

- 781 **Almagro Armenteros J, Sønderby CK, Sønderby SK, Nielsen H, Winther O** (2017) DeepLoc:
782 Prediction of protein subcellular localization using deep learning. *Bioinformatics* **33**: 3387–3395
- 783 **Almagro Armenteros J, Tsirigos KD, Sønderby CK, Petersen TN, Winther O, Brunak S,**
784 **Heijne G von, Nielsen H** (2019) SignalP 5.0 improves signal peptide predictions using deep
785 neural networks. *Nature Biotechnology* **37**: 420–423
- 786 **Banerjee R, Gouda H, Pillay S** (2021) Redox-linked coordination chemistry directs vitamin B₁₂
787 trafficking. *Accounts of Chemical Research* **54**: 2003–2013
- 788 **Beedholm-Ebsen R, Wetering KVD, Hardlei T, Nexø E, Borst P, Søren K, Moestrup SK**
789 (2010) Identification of multidrug resistance protein 1 (MRP1/ABCC1) as a molecular gate for
790 cellular export of cobalamin. *Blood* **115**: 1632–1639
- 791 **Bertrand EM, Saito MA, Rose JM, Riesselman CR, Lohan MC, Noble AE, Lee PA, DiTullio**
792 **GR** (2011) Vitamin B₁₂ and iron colimitation of phytoplankton growth in the Ross Sea. *Limonol*
793 *Oceanogr* **52**: 1079-1093
- 794 **Bertrand EM, Allen AE, Dupont CL, Norden-Krichmar TM, Bai J, Valas RE, Saito MA**
795 (2012) Influence of cobalamin scarcity on diatom molecular physiology and identification of a
796 cobalamin acquisition protein. *Proc Natl Acad Sci U S A* **109**: E1762–71
- 797 **Borths EL, Locher KP, Lee AT, Rees DC** (2002) The structure of *Escherichia coli* BtuF and
798 binding to its cognate ATP binding cassette transporter. *Proc Natl Acad Sci U S A* **99**: 16642–7
- 799 **Bunbury F, Helliwell KE, Mehrshahi P, Davey MP, Salmon DL, Holzer A, Smirnov N,**
800 **Smith AG** (2020) Responses of a newly evolved auxotroph of *Chlamydomonas* to B₁₂
801 deprivation. *Plant Physiology* **183**: 167–178
- 802 **Bykov YS, Schaffer M, Dodonova SO, Albert S, Plitzko JM, Baumeister W, Engel BD,**
803 **Briggs JA** (2017) The structure of the COPI coat determined within the cell. *eLife* **6**: e32493
- 804 **Carlucci FA, Silbernagel BS, McNally MP** (2007) The influence of temperature and solar
805 radiation on persistence of vitamin B₁₂, thiamine, and biotin in seawater. *Journal of Phycology* **5**:
806 302–305
- 807 **Choi CC, Ford RC** (2021) ATP binding cassette importers in eukaryotic organisms. *Biological*
808 *Reviews* **96**: 1318–1330
- 809 **Coelho D, Kim JC, Miousse IR, Fung S, Moulin M du, Buers I, Suormala T, Burda P,**
810 **Frapolli M, Stucki M, et al** (2012) Mutations in ABCD4 cause a new inborn error of vitamin
811 B₁₂ metabolism. *Nature Genetics* **44**: 1152–1155
- 812 **Craig RJ, Hasan AR, Ness RW, Keightley PD** (2021) Comparative genomics of
813 *Chlamydomonas*. *Plant Cell* **33**:1016-1041
- 814 **Croft MT, Lawrence AD, Raux-Deery E, Warren MJ, Smith AG** (2005) Algae acquire
815 vitamin B₁₂ through a symbiotic relationship with bacteria. *Nature* **438**: 90–3
- 816 **Crozet P, Navarro FJ, Willmund F, Mehrshahi P, Bakowski K, Lauersen KJ, Pérez-Pérez**
817 **M-E, Auroy P, Gorchs Rovira A, Sauret-Gueto S, et al** (2018) Birth of a photosynthetic
818 chassis: A MoClo toolkit enabling synthetic biology in the microalga *Chlamydomonas*
819 *reinhardtii*. *ACS Synthetic Biology* **7**: 2074–2086
- 820 **Denning GM, Fulton AB** (1989) Purification and characterization of clathrin-coated vesicles
821 from *Chlamydomonas*. *The Journal of Protozoology* **36**: 334–340

- 822 **Droop MR** (1968) Vitamin B₁₂ and marine ecology. IV. The kinetics of uptake, growth and
823 inhibition in *Monochrysis lutheri*. Journal of the Marine Biological Association of the United
824 Kingdom **48**: 689–733
- 825 **Field CB, Behrenfeld MJ, Randerson JT, Falkowski P** (1998) Primary production of the
826 biosphere: Integrating terrestrial and oceanic components. Science **281**: 237–240
- 827 **Gonzalez JC, Banerjee RV, Huang S, Sumner JS, Matthews RG** (1992) Comparison of
828 cobalamin-independent and cobalamin-dependent methionine synthases from *Escherichia coli*:
829 Two solutions to the same chemical problem. Biochemistry **31**: 6045–6056
- 830 **Goold HD, Cuiné S, Légeret B, Liang Y, Brugière S, Auroy P, Javot H, Tardif M, Jones B,**
831 **Beisson F, et al** (2016) Saturating light induces sustained accumulation of oil in plastidal lipid
832 droplets in *Chlamydomonas reinhardtii*. Plant Physiology **171**: 2406–2417
- 833 **Hanson AD, Roje S** (2001) One-Carbon metabolism in higher plants. Ann Rev Plant Physiol **52**:
834 119–137
- 835 **Helliwell KE, Collins S, Kazamia E, Purton S, Wheeler GL, Smith AG** (2015) Fundamental
836 shift in vitamin B₁₂ eco-physiology of a model alga demonstrated by experimental evolution.
837 ISME J **9**: 1446–1455
- 838 **Helliwell KE, Scaife MA, Sasso S, Araujo APU, Purton S, Smith AG** (2014) Unraveling
839 vitamin B₁₂-responsive gene regulation in algae. Plant Physiol **165**: 388–397
- 840 **Helliwell KE, Wheeler GL, Leptos KC, Goldstein RE, Smith AG** (2011) Insights into the
841 evolution of vitamin B₁₂ auxotrophy from sequenced algal genomes. Molecular Biology and
842 Evolution **28**: 2921–2933
- 843 **Hopes A, Nekrasov V, Belshaw N, Grouneva I, Kamoun S, Mock T** (2017) Genome editing in
844 diatoms using CRISPR-cas to induce precise bi-allelic deletions. Bio Protoc **7**: e2625
- 845 **Joglar V, Pontiller B, Martínez-García S, Fuentes-Lema A, Pérez-Lorenzo M, Lundin D,**
846 **Pinhassi J Fernández E, Teira E** (2021) Microbial plankton community structure and function
847 responses to vitamin B₁₂ and B₁ amendments in an upwelling system. Appl Environ Microbiol **87**:
848 e0152521.
- 849 **Kadner RJ** (1990) Vitamin B₁₂ transport in *Escherichia coli*: Energy coupling between
850 membranes. Molecular Microbiology **4**: 2027–2033
- 851 **Katoh K, Standley DM** (2013) MAFFT multiple sequence alignment software version 7:
852 Improvements in performance and usability. Molecular Biology and Evolution **30**: 772–780
- 853 **King N, Westbrook MJ, Young SL, Kuo A, Abedin M, Chapman J, et al.** (2008). The
854 genome of the choanoflagellate *Monosiga brevicollis* and the origin of metazoans. Nature. **451**:
855 783–788.
- 856 **Koch F, Hattenrath-Lehmann TK, Goleski JA, Sañudo-Wilhelmy S, Fisher NS, Gobler CJ.**
857 **2012.** Vitamin B₁ and B₁₂ uptake and cycling by plankton communities in coastal
858 ecosystems. Front Microbiol **3**:363.
- 859 **Lawrence AD, Nemoto-Smith E, Deery E, Baker JA, Schroeder S, Brown DG, Tullet JMA,**
860 **Howard MJ, Brown IR, Smith AG, et al** (2018) Construction of fluorescent analogs to follow
861 the uptake and distribution of cobalamin (vitamin B₁₂) in bacteria, worms, and plants. Cell Chem
862 Biol **25**: 941–951

- 863 **Li X, Zhang R, Patena W, Gang SS, Blum SR, Ivanova N, Yue R, Robertson JM, Lefebvre**
864 **PA, Fitz-Gibbon ST, et al** (2016) An indexed, mapped mutant library enables reverse genetics
865 studies of biological processes in *Chlamydomonas reinhardtii*. *Plant Cell* **28**: 367–87
- 866 **Mackinder LCM, Chen C, Leib RD, Patena W, Blum SR, Rodman M, Ramundo S, Adams**
867 **CM, Jonikas MC** (2017) A spatial interactome reveals the protein organization of the algal CO₂
868 concentrating mechanism. *Cell* **171**: 133–147.e14
- 869 **Manni M, Berkeley MR, Seppely M, Simão FA, Zdobnov EM** (2021) BUSCO update: Novel
870 and streamlined workflows along with broader and deeper phylogenetic coverage for scoring of
871 eukaryotic, prokaryotic, and viral genomes. *Molecular Biology and Evolution* **38**: 4647–4654
- 872 **Mehrshahi P, Nguyen GTDT, Gorchs Rovira A, Sayer A, Llaveró-Pasquina M, Lim Huei**
873 **Sin M, Medcalf EJ, Mendoza-Ochoa GI, Scaife MA, Smith AG** (2020) Development of novel
874 riboswitches for synthetic biology in the green alga *Chlamydomonas*. *ACS Synthetic Biology* **9**:
875 1406–1417
- 876 **Mentch SJ, Locasale JW** (2016) One-carbon metabolism and epigenetics: understanding the
877 specificity *Ann NY Acad Sci* **1363**: 91-8
- 878 **Mitchell AL, Attwood TK, Babbitt PC, Blum M, Bork P, Bridge A, Brown SD, Chang H-Y,**
879 **El-Gebali S, Fraser MI et al.** (2019) InterPro in 2019: improving coverage, classification and
880 access to protein sequence annotations. *Nucl Acids Res* **47**: D351–D360
- 881 **Neupert J, Karcher D, Bock R** (2009) Generation of *Chlamydomonas* strains that efficiently
882 express nuclear transgenes. *The Plant Journal* **57**: 1140–1150
- 883 **Nielsen MJ, Rasmussen MR, Andersen CBF, Nexø E, Moestrup SK** (2012) Vitamin B₁₂
884 transport from food to the body's cells—a sophisticated, multistep pathway. *Nature Reviews*
885 *Gastroenterology & Hepatology* **9**: 345–354
- 886 **Ohwada K** (1973) Seasonal cycles of vitamin B₁₂, thiamine and biotin in Lake Sagami. Patterns
887 of their distribution and ecological significance. *Internationale Revue der gesamten*
888 *Hydrobiologie und Hydrographie* **58**: 851–871
- 889 **Orłowska M, Steczkiewicz K, Muszewska A** (2021) Utilization of cobalamin is ubiquitous in
890 early-branching fungal phyla. *Genome Biology and Evolution* **13**: evab043
- 891 **Panzeca C, Beck AJ, Tovar-Sanchez A, Segovia-Zavala J, Taylor GT, Gobler CJ, Sañudo-**
892 **Wilhelmy SA** (2009) Distributions of dissolved vitamin B₁₂ and Co in coastal and open-ocean
893 environments. *Estuarine, Coastal and Shelf Science* **85**: 223–230
- 894 **Pintner IJ, Altmeyer VL** (1979) Vitamin B₁₂-binder and other algal inhibitors. *Journal of*
895 *Phycology* **15**: 391–398
- 896 **Richter DJ, Berney C, Strassert JFH, Poh Y-P, Herman EK, Muñoz-Gómez SA, Wideman**
897 **JG, Burki F, Vargas C de** (2022) EukProt: A database of genome-scale predicted proteins across
898 the diversity of eukaryotes. *Peer Community Journal* **2**: e56
- 899 **Ritz C, Baty F, Streibig JC, Gerhard D** (2015) Dose-response analysis using R. *PLoS One* **10**:
900 e0146021
- 901 **Rutsch F, Gailus S, Miousse IR, Suormala T, Sagné C, Toliat MR, Nürnberg G, Wittkamp**
902 **T, Buers I, Sharifi A, et al** (2009) Identification of a putative lysosomal cobalamin exporter
903 altered in the cblF defect of vitamin B₁₂ metabolism. *Nature Genetics* **41**: 234–239
- 904 **Sahni MK, Spanos S, Wahrman MZ, Sharma GM** (2001) Marine corrinoid-binding proteins
905 for the direct determination of vitamin B₁₂ by radioassay. *Analytical Biochemistry* **289**: 68–76

- 906 **Sañudo-Wilhelmy SA, Gómez-Consarnau L, Suffridge C, Webb EA** (2014) The role of B
907 vitamins in marine biogeochemistry. *Annual Review of Marine Science* **6**: 339–367
- 908 **Shelton AN, Seth EC, Mok KC, Han AW, Jackson SN, Haft DR, Taga ME** (2019) Uneven
909 distribution of cobamide biosynthesis and dependence in bacteria predicted by comparative
910 genomics. *The ISME Journal* **13**: 789–804
- 911 **Tang YZ, Koch F, Gobler CJ** (2010) Most harmful algal bloom species are vitamin B₁ and B₁₂
912 auxotrophs. *Proc Natl Acad Sci U S A* **107**: 20756–61
- 913 **Warren MJ, Raux E, Schubert HL, Escalante-Semerena JC** (2002) The biosynthesis of
914 adenosylcobalamin (vitamin B₁₂). *Natural product reports* **19**: 390–412
- 915 **Xie B, Bishop S, Stessman D, Wright D, Spalding MH, Halverson LJ** (2013) *Chlamydomonas*
916 *reinhardtii* thermal tolerance enhancement mediated by a mutualistic interaction with vitamin B₁₂-
917 producing bacteria. *ISME J* **7**: 1544–55
- 918 **Yu Z, Geisler K, Leontidou T, Young REB, Vonlanthen SE, Purton S, Abell C, Smith AG**
919 (2021) Droplet-based microfluidic screening and sorting of microalgal populations for strain
920 engineering applications. *Algal Res* **56**: 102293
- 921
- 922
- 923
- 924
- 925

ACCEPTED MANUSCRIPT

Figure 1

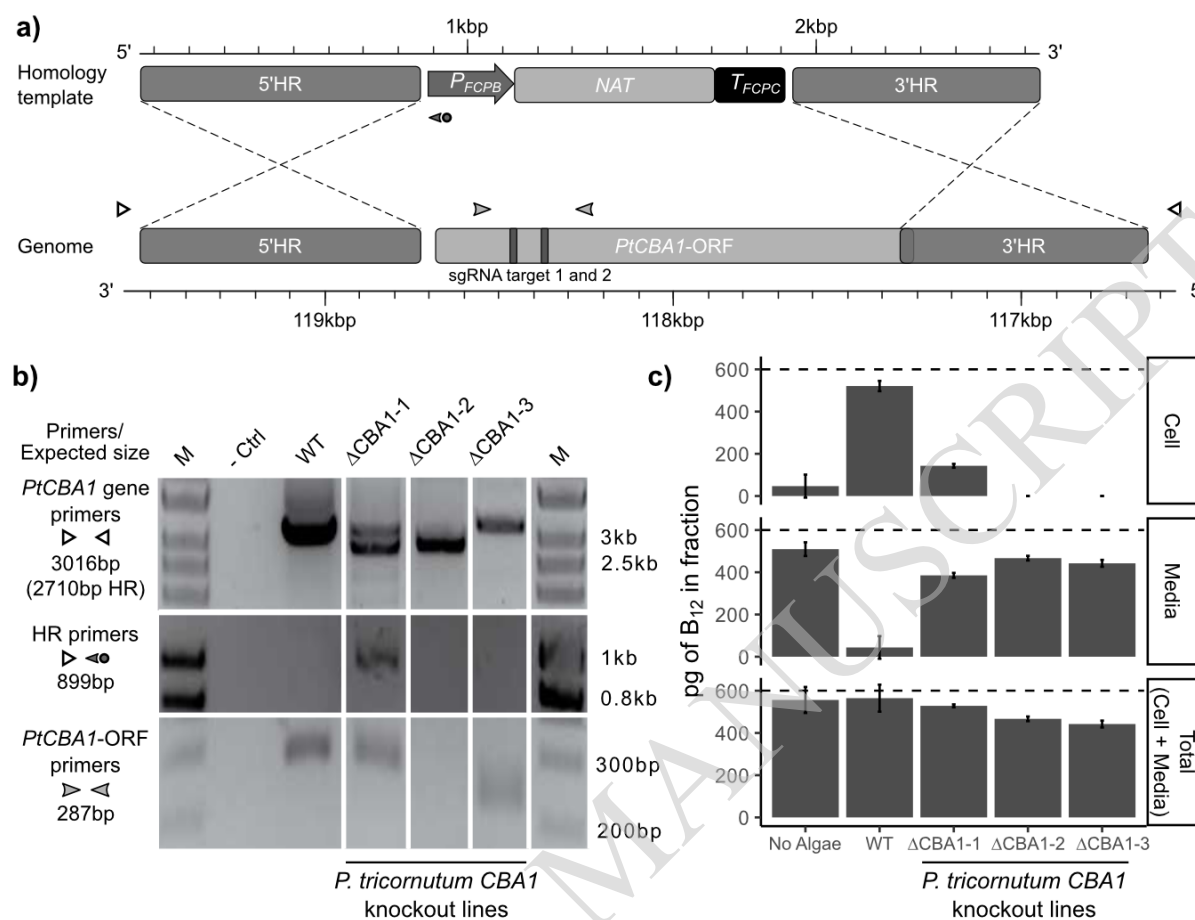


Figure 1. Disruption of *Phaeodactylum tricornutum* CBA1 (*PtCBA1*) using CRISPR-Cas9 yielded lines with impaired B_{12} uptake. a) Schematic showing CRISPR-Cas9 sgRNA target sites and the homology repair template design used to generate mutant lines in *PtCBA1* (Phatr3_J48322). The homology repair template schematic is annotated with the 5' homology region (HR) and 3'HR, the *FCPB* promoter, nourseothricin resistance gene (*NAT*) and *FCPC* terminator. The *PtCBA1* gene is annotated with the ORF, the 5'HR and 3'HR regions used in the homology template and the regions of the ORF targeted by sgRNA (vertical bars). Primer positions used for the analysis of putative mutant lines are shown with arrowheads. **b)** PCR of regions across and within wild-type (WT) and mutant *PtCBA1* in 3 independent CRISPR-Cas9 lines (Δ CBA1) showing indel mutations in the mutants. PCR products from different sets of primers indicated in panel a are shown. M = marker, - Ctrl = no DNA template. **c)** A B_{12} uptake assay was performed as described in Materials and Methods, to determine the amount of B_{12} in the media and the cells after 1h incubation of *P. tricornutum* cells in 600 pg B_{12} . The 'Total' was inferred by the addition of the cell and media fractions. The dashed line indicates the amount of B_{12} added to the experiment. Standard deviation error bars are shown, n=4. Statistical analysis was performed on the media fraction, and Tukey's test identified the following comparisons to be significantly different from one another: WT vs No Algae ($p < 1e^{-12}$); WT vs Δ CBA1-1 ($p < 1e^{-10}$); WT vs Δ CBA1-2 ($p < 1e^{-12}$); WT vs Δ CBA1-3 ($p < 1e^{-11}$); No Algae vs Δ CBA1-1 ($p < 1e^{-03}$); No Algae vs Δ CBA1-3 ($p < 0.05$); and Δ CBA1-1 vs Δ CBA1-2 ($p < 1e^{-02}$).

Figure 2

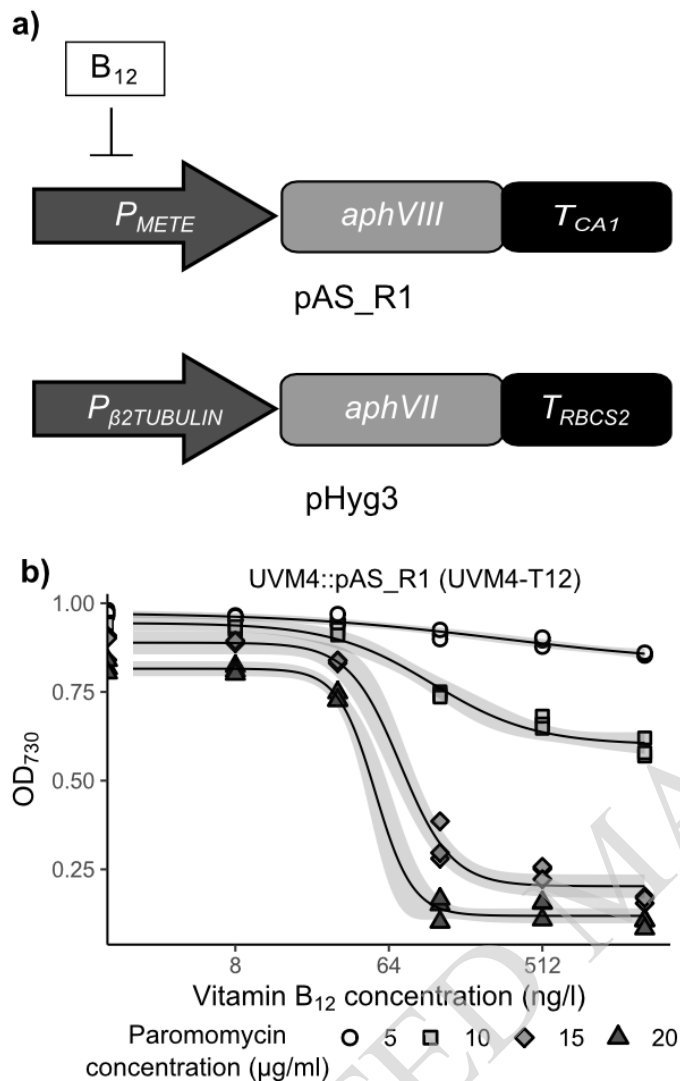


Figure 2. Generation and use of *C. reinhardtii* reporter strain UVM4-T12 for insertional mutagenesis. **a)** Schematic of the constructs used for insertional mutagenesis of *C. reinhardtii*. The pAS_R1 construct was designed to control expression of the paromomycin resistance gene (*aphVIII*) via B₁₂ mediated repression of the *METE* promoter (*P_{METE}*). The pHyg3 construct encoded a constitutively expressed hygromycin resistance gene (*aphVII*), to be used for insertional mutagenesis. **b)** Growth of *C. reinhardtii* B₁₂ reporter strain UVM4-T12 bearing pAS_R1 plasmid, in response to vitamin B₁₂ and paromomycin concentration in the media according to the algal dose-response assay. The predicted dose-response model is shown in black, with 95% confidence intervals in grey.

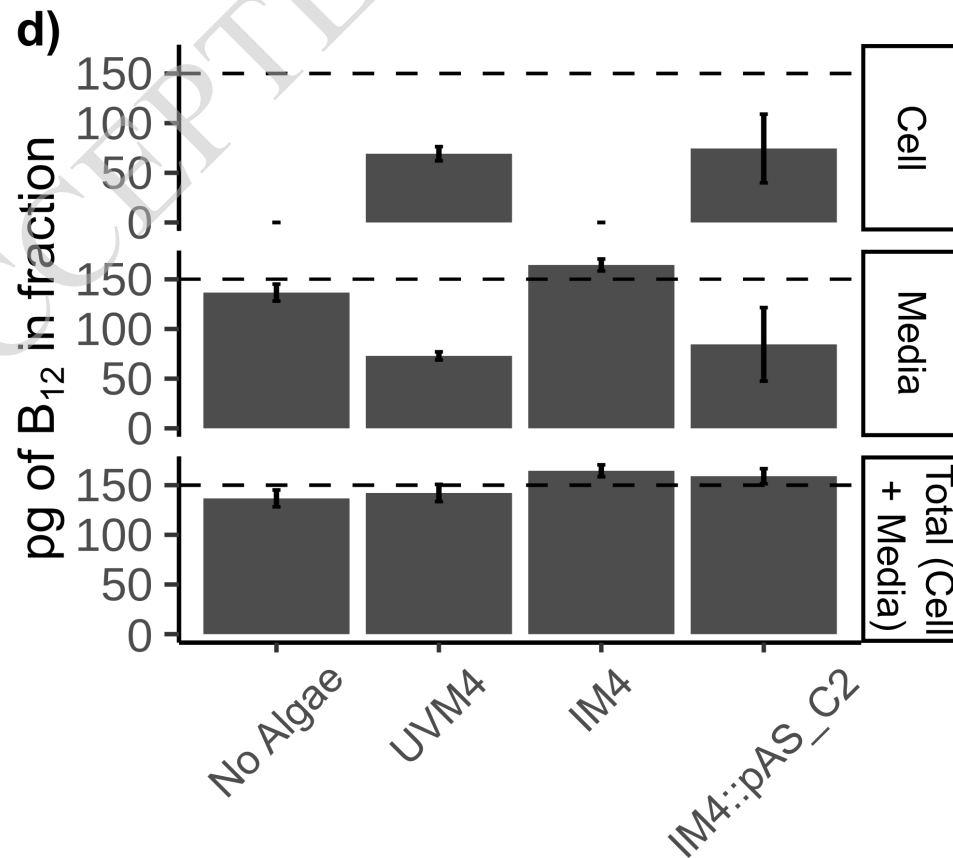
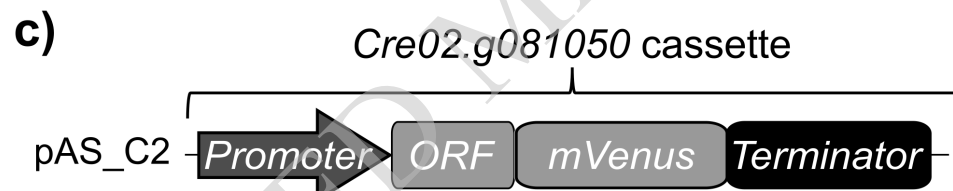
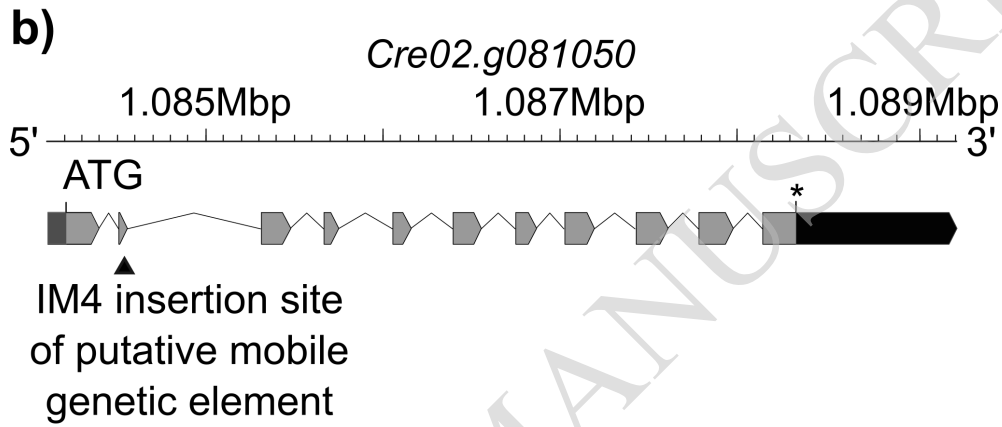
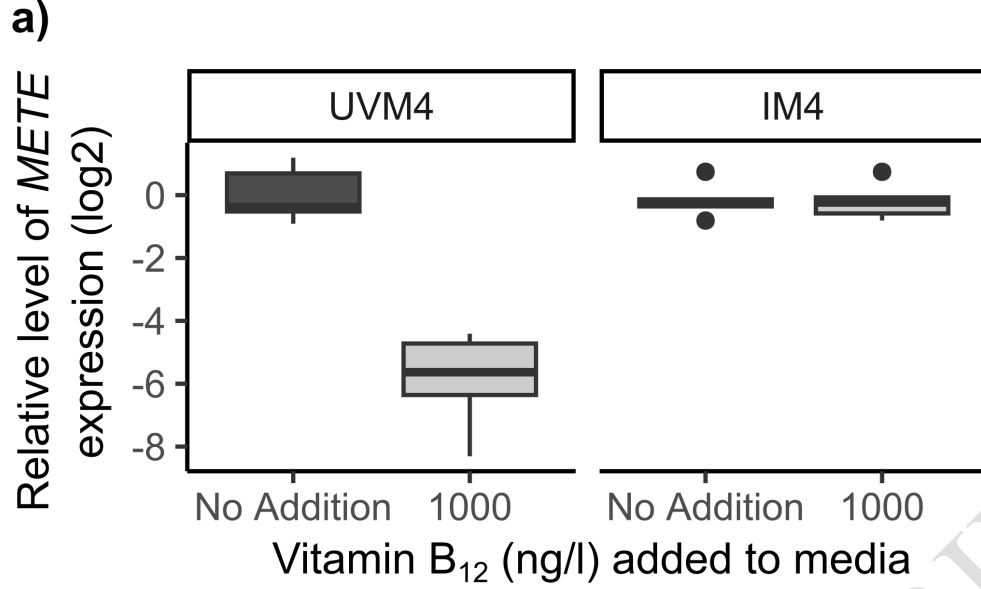


Figure 4

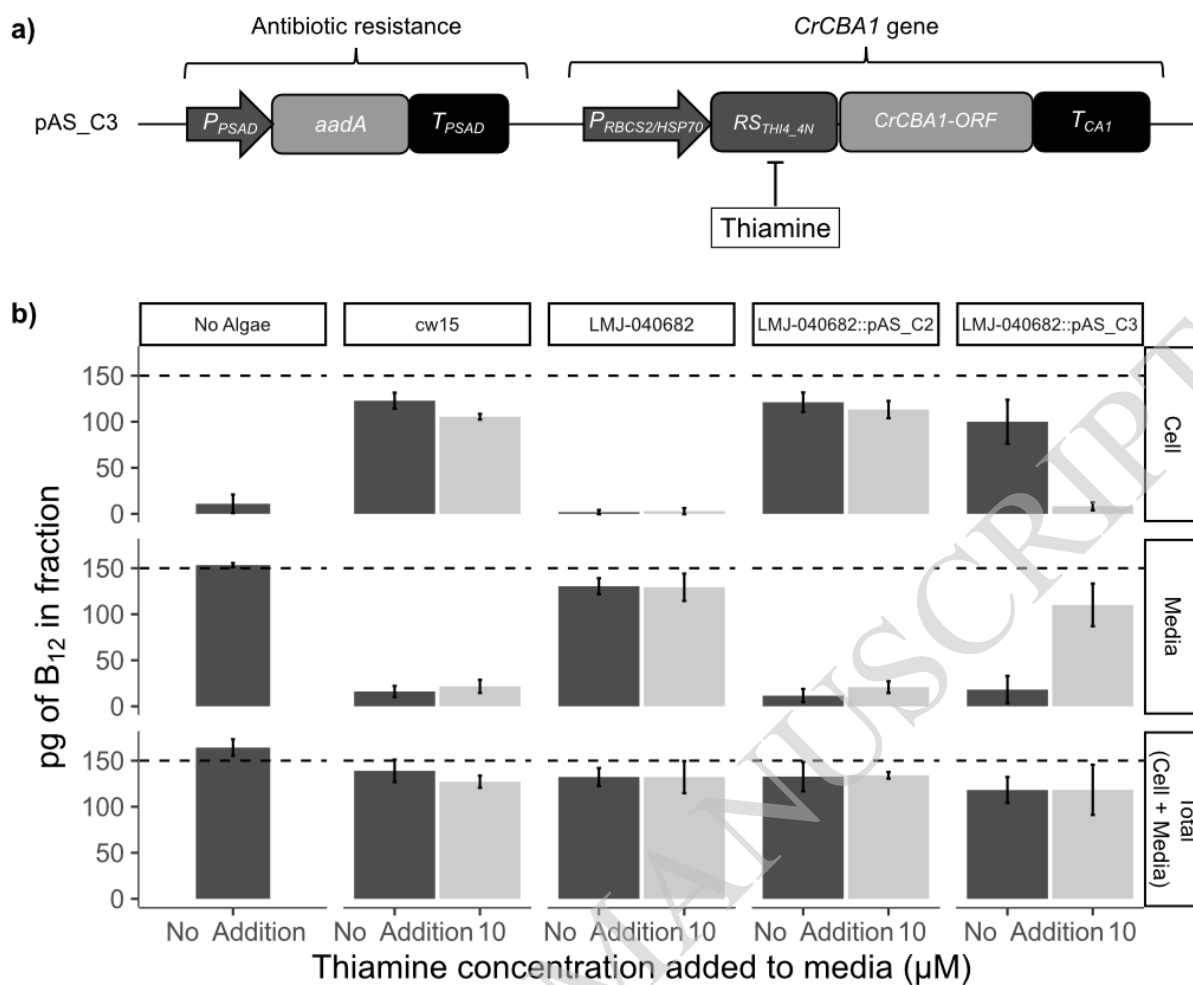


Figure 4. CLiP mutants in CrCBA1 are impaired in their ability to take up B₁₂. **a)**

Schematic of the pAS_C3 construct designed to express *CrCBA1* in a controllable manner using a thiamine repressible riboswitch (RS_{THI4_4N}) to allow repression of *CrCBA1* through the addition of thiamine (Mehrshahi et al., 2020). **b)** B₁₂-uptake assay with cw15, LMJ-040682 and mean of 3 independent transformants of LMJ-040682::pAS_C2 and LMJ-040682::pAS_C3. The growth conditions were modified compared to previous assays: lines were grown with or without 10 μ M thiamine supplementation for 5 days in a 16/8 light/dark cycle, and 8 hours after the dark to light transition the cultures were used for the algal B₁₂-uptake assay. The dashed line indicates the amount of B₁₂ added to the sample. Standard deviation error bars are shown. Statistical analysis was performed on the media fraction. Tukey's test identified the following algal strains to be significantly different from one another in media without thiamine (not reporting comparisons against the No Algae control condition): cw15 vs LMJ-040682 ($p < 1e^{-10}$); LMJ-040682 vs LMJ-040682::pAS_C2 ($p < 1e^{-09}$); and LMJ-040682 vs LMJ-040682::pAS_C3 ($p < 1e^{-09}$). Additionally, Tukey's test found the following strain to show a significant difference due to thiamine addition: LMJ-040682::pAS_C3 ($p < 1e^{-07}$).

Figure 5

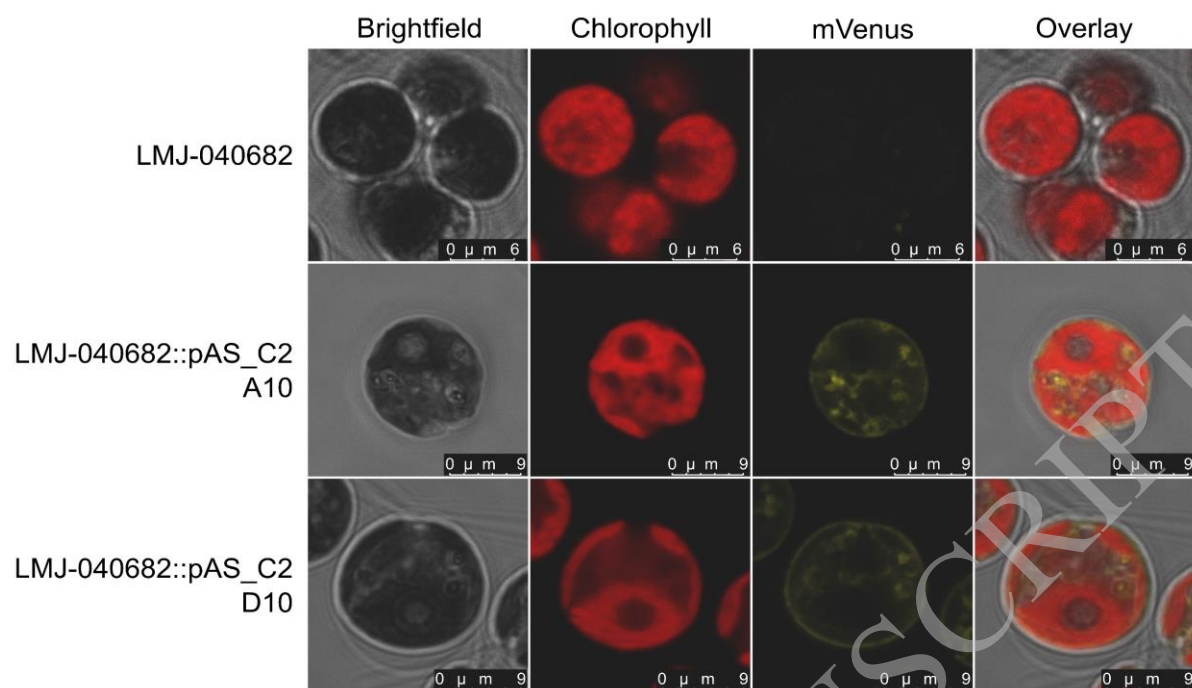


Figure 5. Confocal microscopy of complemented *C. reinhardtii* CrCBA1 knockout lines showing an association between CrCBA1 and membranes. LMJ-040682 and LMJ-040682::pAS_C2 A10 and D10 lines were imaged according to the protocol outlined in the materials and methods. Channels shown (left to right) are brightfield, chlorophyll, mVenus and an overlay. Microscope settings are described in Methods.

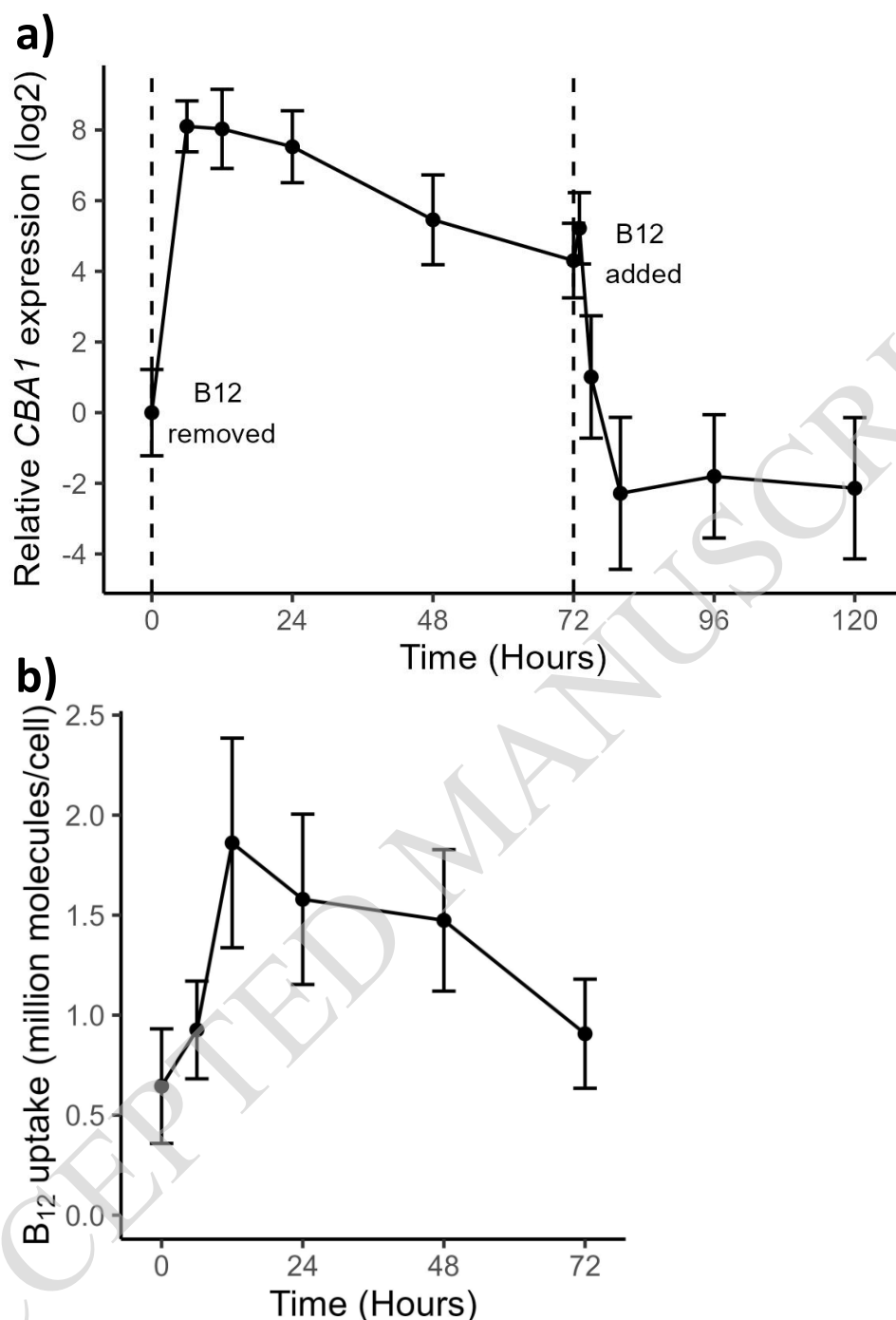


Figure 6. *CBA1* expression and B₁₂ uptake capacity in a B₁₂-dependent mutant of *C. reinhardtii* (*metE7*) during B₁₂ starvation and add-back. a) Log₂-transformed expression level of *CBA1* measured by RT-qPCR and adjusted using the 2^{-ΔΔCt} method (relative to the housekeeping gene *RACK1* and *CBA1* expression at 0 hours). Vertical dashed lines indicate when B₁₂ was removed and added. **b)** B₁₂ uptake capacity of starved *metE7* cells (expressed as 10⁶ molecules of B₁₂ per cell over 1h) at the same six time points during B₁₂ starvation; it was not possible to perform the uptake assay on cells to which B₁₂ had already been added (after 72 hours). Cell density measurements were performed by counting plated cells in dilution series and so included non-viable cells. For *CBA1* expression and B₁₂ uptake, 3 and 6 biological replicates were used, respectively, with points representing means, and error bars representing standard deviations.

Figure 7

| Class (no. of taxa) | | % with METH | % with METH+METE | % with METE |
|-----------------------|---------|-------------|------------------|-------------|
| Chlorophyta (18) | CBA1 | 61 | 17 | 0 |
| | No CBA1 | 11 | 6 | 6 |
| Stramenopiles (48) | CBA1 | 48 | 17 | 2 |
| | No CBA1 | 4 | 21 | 8 |
| Alveolata (11) | CBA1 | 45 | 0 | 0 |
| | No CBA1 | 45 | 0 | 9 |
| Rhizaria (9) | CBA1 | 67 | 0 | 0 |
| | No CBA1 | 11 | 22 | 0 |
| Streptophyta (22) | CBA1 | 0 | 5 | 73 |
| | No CBA1 | 0 | 0 | 23 |
| Amoebozoa (13) | CBA1 | 0 | 8 | 0 |
| | No CBA1 | 31 | 62 | 0 |
| Choanoflagellata (22) | CBA1 | 23 | 0 | 0 |
| | No CBA1 | 77 | 0 | 0 |
| Metazoa (42) | CBA1 | 0 | 0 | 0 |
| | No CBA1 | 83 | 12 | 5 |
| Fungi (27) | CBA1 | 0 | 19 | 7 |
| | No CBA1 | 0 | 4 | 70 |

Figure 7. Distribution of CBA1 and methionine synthase sequences across Eukaryotic groups. The EukProt database (Richter et al., 2022) was searched for METE, METH and CBA1 queries, as described in the materials and methods. Organisms were only considered if they contained at least one valid methionine synthase hit (METE or METH) and their genomes were >70% complete, as measured by BUSCO (Manni et al., 2021). Eukaryotic classes were filtered for those with greater than 5 genomes and the numbers of taxa for each class are indicated in brackets. The different combinations of CBA1, METE and METH were calculated for each species (Supplementary Table 4) and summarised as a percentage of the total number of taxa in each class, with gradual shading to show the variation in distribution between the different classes.

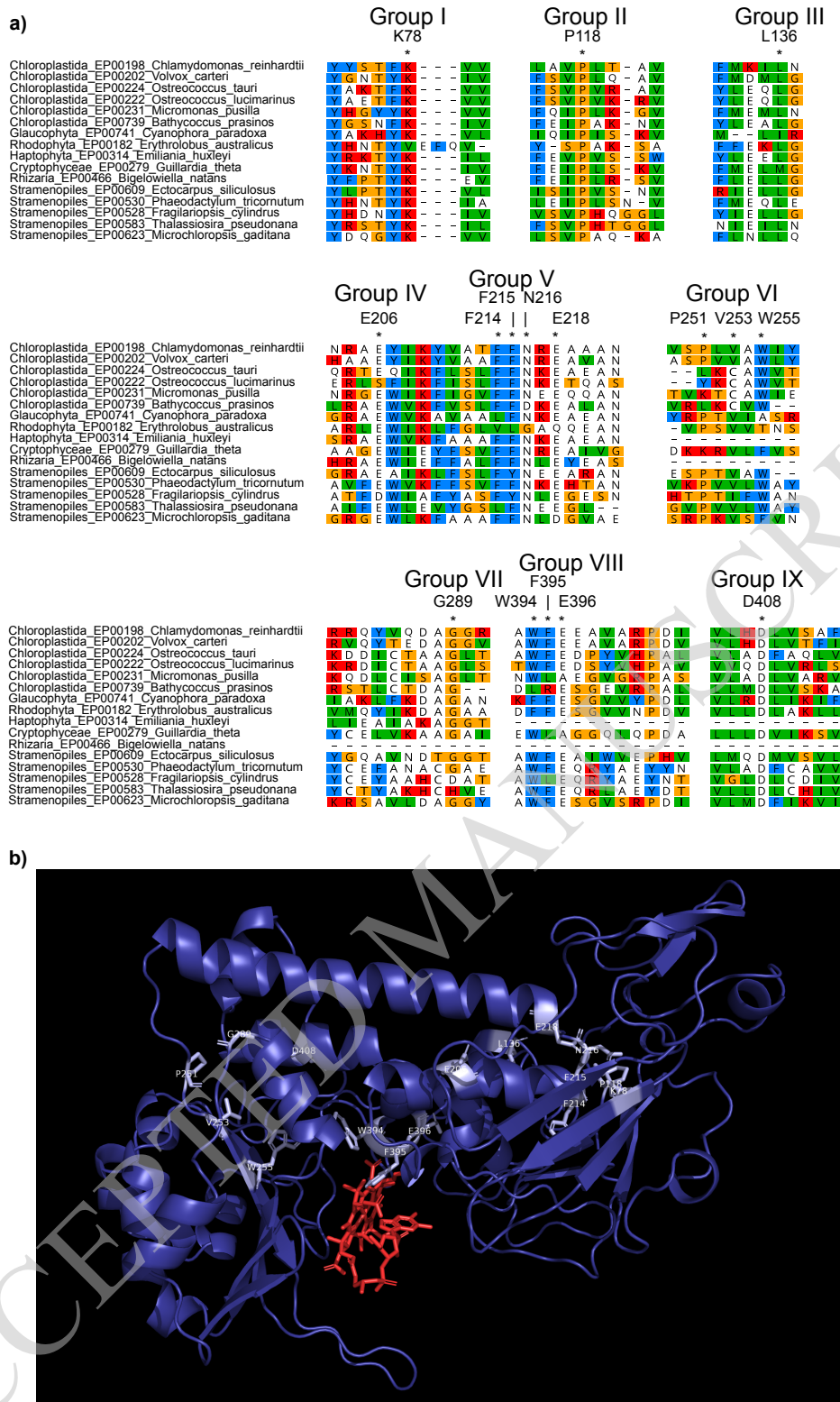


Figure 8. Identification and predicted structural location of CrCBA1 conserved residues. **a)** Sequences with similarity to CBA1 were identified from the EukProt database (Richter et al., 2022) using a manually generated CBA1 Hidden Markov Model (HMM), as described in the materials and methods. A selection of 16 taxa from several eukaryotic supergroups were chosen and conserved regions from the protein are presented. Specific residues indicated by * are: K78, P118, L136, E206, F214, F215, N216, E218, P251, V253, W255, G289, W394, F395, E396 and D408. Protein sequences are coloured according to the Clustal colour-scheme using Geneious Prime 2021.1.1 (www.geneious.com). For each highly conserved region, the corresponding position and amino acid from the CrCBA1 sequence (Cre02.g081050) is indicated. **b)** The predicted 3D structure of CrCBA1 (residues 21-490) was obtained from the AlphaFold Protein Structure Database (entry: A0A2K3E0J7). Highly conserved regions of CrCBA1 are indicated in light blue and labelled. CrCBA1 was aligned to the crystal structure of *E. coli* BtuF in complex with B₁₂ (pdb: 1n2z). This enabled the relative position of B₁₂ (shown in red) to be superimposed onto CrCBA1.

Parsed Citations

Allen, MD, del Campo JA, Kropat J, Merchant SS (2007) FEA1, FEA2, and FRE1, encoding two homologous secreted proteins and a candidate ferrireductase, are expressed coordinately with FOX1 and FTR1 in iron-deficient *Chlamydomonas reinhardtii*. *Eukaryotic Cell* 6: 1841–1852

Google Scholar: [Author Only](#) [Title Only](#) [Author and Title](#)

Almagro Armenteros J, Sønderby CK, Sønderby SK, Nielsen H, Winther O (2017) DeepLoc: Prediction of protein subcellular localization using deep learning. *Bioinformatics* 33: 3387–3395

Google Scholar: [Author Only](#) [Title Only](#) [Author and Title](#)

Almagro Armenteros J, Tsirigos KD, Sønderby CK, Petersen TN, Winther O, Brunak S, Heijne G von, Nielsen H (2019) SignalP 5.0 improves signal peptide predictions using deep neural networks. *Nature Biotechnology* 37: 420–423

Google Scholar: [Author Only](#) [Title Only](#) [Author and Title](#)

Banerjee R, Gouda H, Pillay S (2021) Redox-linked coordination chemistry directs vitamin B12 trafficking. *Accounts of Chemical Research* 54: 2003–2013

Google Scholar: [Author Only](#) [Title Only](#) [Author and Title](#)

Beedholm-Ebsen R, Wetering KVD, Hardlei T, Nexø E, Borst P, Søren K, Moestrup SK (2010) Identification of multidrug resistance protein 1 (MRP1/ABCC1) as a molecular gate for cellular export of cobalamin. *Blood* 115: 1632–1639

Google Scholar: [Author Only](#) [Title Only](#) [Author and Title](#)

Bertrand EM, Saito MA, Rose JM, Riesselman CR, Lohan MC, Noble AE, Lee PA, DiTullio GR (2011) Vitamin B12 and iron colimitation of phytoplankton growth in the Ross Sea. *Limnol Oceanogr* 52: 1079–1093

Google Scholar: [Author Only](#) [Title Only](#) [Author and Title](#)

Bertrand EM, Allen AE, Dupont CL, Norden-Krichmar TM, Bai J, Valas RE, Saito MA (2012) Influence of cobalamin scarcity on diatom molecular physiology and identification of a cobalamin acquisition protein. *Proc Natl Acad Sci U S A* 109: E1762–71

Google Scholar: [Author Only](#) [Title Only](#) [Author and Title](#)

Borths EL, Locher KP, Lee AT, Rees DC (2002) The structure of *Escherichia coli* BtuF and binding to its cognate ATP binding cassette transporter. *Proc Natl Acad Sci U S A* 99: 16642–7

Google Scholar: [Author Only](#) [Title Only](#) [Author and Title](#)

Bunbury F, Helliwell KE, Mehrshahi P, Davey MP, Salmon DL, Holzer A, Smirnov N, Smith AG (2020) Responses of a newly evolved auxotroph of *Chlamydomonas* to B12 deprivation. *Plant Physiology* 183: 167–178

Google Scholar: [Author Only](#) [Title Only](#) [Author and Title](#)

Bykov YS, Schaffer M, Dodonova SO, Albert S, Plitzko JM, Baumeister W, Engel BD, Briggs JA (2017) The structure of the COPI coat determined within the cell. *eLife* 6: e32493

Google Scholar: [Author Only](#) [Title Only](#) [Author and Title](#)

Carlucci FA, Silbernagel BS, McNally MP (2007) The influence of temperature and solar radiation on persistence of vitamin B12, thiamine, and biotin in seawater. *Journal of Phycology* 5: 302–305

Google Scholar: [Author Only](#) [Title Only](#) [Author and Title](#)

Choi CC, Ford RC (2021) ATP binding cassette importers in eukaryotic organisms. *Biological Reviews* 96: 1318–1330

Google Scholar: [Author Only](#) [Title Only](#) [Author and Title](#)

Coelho D, Kim JC, Miousse IR, Fung S, Moulin M du, Buers I, Suormala T, Burda P, Frapolli M, Stucki M, et al (2012) Mutations in ABCD4 cause a new inborn error of vitamin B12 metabolism. *Nature Genetics* 44: 1152–1155

Google Scholar: [Author Only](#) [Title Only](#) [Author and Title](#)

Craig RJ, Hasan AR, Ness RW, Keightley PD (2021) Comparative genomics of *Chlamydomonas*. *Plant Cell* 33:1016–1041

Google Scholar: [Author Only](#) [Title Only](#) [Author and Title](#)

Croft MT, Lawrence AD, Raux-Deery E, Warren MJ, Smith AG (2005) Algae acquire vitamin B12 through a symbiotic relationship with bacteria. *Nature* 438: 90–3

Google Scholar: [Author Only](#) [Title Only](#) [Author and Title](#)

Crozet P, Navarro FJ, Willmund F, Mehrshahi P, Bakowski K, Lauersen KJ, Pérez-Pérez M-E, Auroy P, Gorchs Rovira A, Sauret-Gueto S, et al (2018) Birth of a photosynthetic chassis: A MoClo toolkit enabling synthetic biology in the microalga *Chlamydomonas reinhardtii*. *ACS Synthetic Biology* 7: 2074–2086

Google Scholar: [Author Only](#) [Title Only](#) [Author and Title](#)

Denning GM, Fulton AB (1989) Purification and characterization of clathrin-coated vesicles from *Chlamydomonas*. *The Journal of Protozoology* 36: 334–340

Google Scholar: [Author Only](#) [Title Only](#) [Author and Title](#)

Droop MR (1968) Vitamin B12 and marine ecology. IV. The kinetics of uptake, growth and inhibition in *Monochrysis lutheri*. *Journal of the Marine Biological Association of the United Kingdom* 48: 689–733

Google Scholar: [Author Only](#) [Title Only](#) [Author and Title](#)

Field CB, Behrenfeld MJ, Randerson JT, Falkowski P (1998) Primary production of the biosphere: Integrating terrestrial and oceanic components. *Science* 281: 237–240

Google Scholar: [Author Only](#) [Title Only](#) [Author and Title](#)

Gonzalez JC, Banerjee RV, Huang S, Sumner JS, Matthews RG (1992) Comparison of cobalamin-independent and cobalamin-dependent methionine synthases from *Escherichia coli*: Two solutions to the same chemical problem. *Biochemistry* 31: 6045–6056

Google Scholar: [Author Only](#) [Title Only](#) [Author and Title](#)

Goold HD, Cuiñé S, Légeret B, Liang Y, Brugière S, Auroy P, Javot H, Tardif M, Jones B, Beisson F, et al (2016) Saturating light induces sustained accumulation of oil in plastidal lipid droplets in *Chlamydomonas reinhardtii*. *Plant Physiology* 171: 2406–2417

Google Scholar: [Author Only](#) [Title Only](#) [Author and Title](#)

Hanson AD, Roje S (2001) One-Carbon metabolism in higher plants. *Ann Rev Plant Physiol* 52: 119-137

Google Scholar: [Author Only](#) [Title Only](#) [Author and Title](#)

Helliwell KE, Collins S, Kazamia E, Purton S, Wheeler GL, Smith AG (2015) Fundamental shift in vitamin B12 eco-physiology of a model alga demonstrated by experimental evolution. *ISME J* 9: 1446–1455

Google Scholar: [Author Only](#) [Title Only](#) [Author and Title](#)

Helliwell KE, Scaife MA, Sasso S, Araujo APU, Purton S, Smith AG (2014) Unraveling vitamin B12-responsive gene regulation in algae. *Plant Physiol* 165: 388–397

Google Scholar: [Author Only](#) [Title Only](#) [Author and Title](#)

Helliwell KE, Wheeler GL, Leptos KC, Goldstein RE, Smith AG (2011) Insights into the evolution of vitamin B12 auxotrophy from sequenced algal genomes. *Molecular Biology and Evolution* 28: 2921–2933

Google Scholar: [Author Only](#) [Title Only](#) [Author and Title](#)

Hopes A, Nekrasov V, Belshaw N, Grouneva I, Kamoun S, Mock T (2017) Genome editing in diatoms using CRISPR-cas to induce precise bi-allelic deletions. *Bio Protoc* 7: e2625

Google Scholar: [Author Only](#) [Title Only](#) [Author and Title](#)

Joglar V, Pontiller B, Martínez-García S, Fuentes-Lema A, Pérez-Lorenzo M, Lundin D, Pinhassi J Fernández E, Teira E (2021) Microbial plankton community structure and function responses to vitamin B12 and B1 amendments in an upwelling system. *Appl Environ Microbiol* 87: e0152521.

Google Scholar: [Author Only](#) [Title Only](#) [Author and Title](#)

Kadner RJ (1990) Vitamin B12 transport in *Escherichia coli*: Energy coupling between membranes. *Molecular Microbiology* 4: 2027–2033

Google Scholar: [Author Only](#) [Title Only](#) [Author and Title](#)

Katoh K, Standley DM (2013) MAFFT multiple sequence alignment software version 7: Improvements in performance and usability. *Molecular Biology and Evolution* 30: 772–780

Google Scholar: [Author Only](#) [Title Only](#) [Author and Title](#)

King N, Westbrook MJ, Young SL, Kuo A, Abedin M, Chapman J, et al. (2008). The genome of the choanoflagellate *Monosiga brevicollis* and the origin of metazoans. *Nature*. 451: 783–788.

Google Scholar: [Author Only](#) [Title Only](#) [Author and Title](#)

Koch F, Hattenrath-Lehmann TK, Goleski JA, Sañudo-Wilhelmy S, Fisher NS, Gobler CJ. 2012. Vitamin B1 and B12 uptake and cycling by plankton communities in coastal ecosystems. *Front Microbiol* 3:363.

Google Scholar: [Author Only](#) [Title Only](#) [Author and Title](#)

Lawrence AD, Nemoto-Smith E, Deery E, Baker JA, Schroeder S, Brown DG, Tullet JMA, Howard MJ, Brown IR, Smith AG, et al (2018) Construction of fluorescent analogs to follow the uptake and distribution of cobalamin (vitamin B12) in bacteria, worms, and plants. *Cell Chem Biol* 25: 941–951

Google Scholar: [Author Only](#) [Title Only](#) [Author and Title](#)

Li X, Zhang R, Patena W, Gang SS, Blum SR, Ivanova N, Yue R, Robertson JM, Lefebvre PA, Fitz-Gibbon ST, et al (2016) An indexed, mapped mutant library enables reverse genetics studies of biological processes in *Chlamydomonas reinhardtii*. *Plant Cell* 28: 367–87

Google Scholar: [Author Only](#) [Title Only](#) [Author and Title](#)

Mackinder LCM, Chen C, Leib RD, Patena W, Blum SR, Rodman M, Ramundo S, Adams CM, Jonikas MC (2017) A spatial interactome reveals the protein organization of the algal CO2 concentrating mechanism. *Cell* 171: 133–147.e14

Google Scholar: [Author Only](#) [Title Only](#) [Author and Title](#)

Manni M, Berkeley MR, Seppey M, Simão FA, Zdobnov EM (2021) BUSCO update: Novel and streamlined workflows along with broader and deeper phylogenetic coverage for scoring of eukaryotic, prokaryotic, and viral genomes. *Molecular Biology and Evolution* 38: 4647–4654

Google Scholar: [Author Only](#) [Title Only](#) [Author and Title](#)

Mehrshahi P, Nguyen GTDT, Gorchs Rovira A, Sayer A, Llaveró-Pasquina M, Lim Huei Sin M, Medcalf EJ, Mendoza-Ochoa GI, Scaife MA, Smith AG (2020) Development of novel riboswitches for synthetic biology in the green alga *Chlamydomonas*. *ACS Synthetic Biology* 9: 1406–1417

Google Scholar: [Author Only](#) [Title Only](#) [Author and Title](#)

Mentch SJ, Locasale JW (2016) One-carbon metabolism and epigenetics: understanding the specificity *Ann NY Acad Sci* 1363: 91-8

Google Scholar: [Author Only](#) [Title Only](#) [Author and Title](#)

Mitchell AL, Attwood TK, Babbitt PC, Blum M, Bork P, Bridge A, Brown SD, Chang H-Y, El-Gebali S, Fraser MI et al. (2019) InterPro in 2019: improving coverage, classification and access to protein sequence annotations. *Nucl Acids Res* 47: D351–D360

Google Scholar: [Author Only](#) [Title Only](#) [Author and Title](#)

Neupert J, Karcher D, Bock R (2009) Generation of *Chlamydomonas* strains that efficiently express nuclear transgenes. *The Plant Journal* 57: 1140–1150

Google Scholar: [Author Only](#) [Title Only](#) [Author and Title](#)

Nielsen MJ, Rasmussen MR, Andersen CBF, Nexø E, Moestrup SK (2012) Vitamin B12 transport from food to the body's cells—a sophisticated, multistep pathway. *Nature Reviews Gastroenterology & Hepatology* 9: 345–354

Google Scholar: [Author Only](#) [Title Only](#) [Author and Title](#)

Ohwada K (1973) Seasonal cycles of vitamin B12, thiamine and biotin in Lake Sagami. Patterns of their distribution and ecological significance. *Internationale Revue der gesamten Hydrobiologie und Hydrographie* 58: 851–871

Google Scholar: [Author Only](#) [Title Only](#) [Author and Title](#)

Orłowska M, Steczkiewicz K, Muszewska A (2021) Utilization of cobalamin is ubiquitous in early-branching fungal phyla. *Genome Biology and Evolution* 13: evab043

Google Scholar: [Author Only](#) [Title Only](#) [Author and Title](#)

Panzeca C, Beck AJ, Tovar-Sanchez A, Segovia-Zavala J, Taylor GT, Gobler CJ, Sañudo-Wilhelmy SA (2009) Distributions of dissolved vitamin B12 and Co in coastal and open-ocean environments. *Estuarine, Coastal and Shelf Science* 85: 223–230

Google Scholar: [Author Only](#) [Title Only](#) [Author and Title](#)

Pintner IJ, Altmeyer VL (1979) Vitamin B12-binder and other algal inhibitors *Journal of Phycology* 15: 391–398

Richter DJ, Berney C, Strassert JFH, Poh Y-P, Herman EK, Muñoz-Gómez SA, Wideman JG, Burki F, Vargas C de (2022) EukProt: A database of genome-scale predicted proteins across the diversity of eukaryotes. *Peer Community Journal* 2: e56

Google Scholar: [Author Only](#) [Title Only](#) [Author and Title](#)

Ritz C, Baty F, Streibig JC, Gerhard D (2015) Dose-response analysis using R. *PLoS One* 10: e0146021

Google Scholar: [Author Only](#) [Title Only](#) [Author and Title](#)

Rutsch F, Gailus S, Miousse IR, Suomalainen T, Sagné C, Toliat MR, Nürnberg G, Wittkamp T, Buers I, Sharifi A, et al (2009) Identification of a putative lysosomal cobalamin exporter altered in the cblF defect of vitamin B12 metabolism. *Nature Genetics* 41: 234–239

Google Scholar: [Author Only](#) [Title Only](#) [Author and Title](#)

Sahni MK, Spanos S, Wahrman MZ, Sharma GM (2001) Marine corrinoid-binding proteins for the direct determination of vitamin B12 by radioassay. *Analytical Biochemistry* 289: 68–76

Google Scholar: [Author Only](#) [Title Only](#) [Author and Title](#)

Sañudo-Wilhelmy SA, Gómez-Consarnau L, Suffridge C, Webb EA (2014) The role of B vitamins in marine biogeochemistry. *Annual Review of Marine Science* 6: 339–367

Google Scholar: [Author Only](#) [Title Only](#) [Author and Title](#)

Shelton AN, Seth EC, Mok KC, Han AW, Jackson SN, Haft DR, Taga ME (2019) Uneven distribution of cobamide biosynthesis and dependence in bacteria predicted by comparative genomics. *The ISME Journal* 13: 789–804

Google Scholar: [Author Only](#) [Title Only](#) [Author and Title](#)

Tang YZ, Koch F, Gobler CJ (2010) Most harmful algal bloom species are vitamin B1 and B12 auxotrophs. *Proc Natl Acad Sci U S A* 107: 20756–61

Google Scholar: [Author Only](#) [Title Only](#) [Author and Title](#)

Warren MJ, Raux E, Schubert HL, Escalante-Semerena JC (2002) The biosynthesis of adenosylcobalamin (vitamin B12). *Natural product reports* 19: 390–412

Google Scholar: [Author Only](#) [Title Only](#) [Author and Title](#)

Xie B, Bishop S, Stessman D, Wright D, Spalding MH, Halverson LJ (2013) Chlamydomonas reinhardtii thermal tolerance enhancement mediated by a mutualistic interaction with vitamin B12-producing bacteria. ISME J 7: 1544–55

Google Scholar: [Author Only](#) [Title Only](#) [Author and Title](#)

Yu Z, Geisler K, Leontidou T, Young REB, Vonlanthen SE, Purton S, Abell C, Smith AG (2021) Droplet-based microfluidic screening and sorting of microalgal populations for strain engineering applications. Algal Res 56: 102293

Google Scholar: [Author Only](#) [Title Only](#) [Author and Title](#)

ACCEPTED MANUSCRIPT